5. FORMULATION DEVELOPMENT AND CHARACTERIZATION

Non-viral vectors are typically cationic materials that condense siRNA by charge interaction (1). The cationic materials commonly comprise either cationic polymers like polyethylenimine (PEI), Poly-L-lysine (PLL) etc. or cationic phospholipids like DOTAP, DOSPA, DOTMA, DOGS etc. (2). Cationic polymers complex with negatively charged siRNA, to form so called polyplexes, through electrostatic interaction between cationic functionalities, typically quaternary ammonium groups and anionic phosphate groups of nucleic acids. Among the cationic polymers, PEI is most commonly evaluated polymer. Among the two forms available (linear and branched), branched PEI of molecular weight of 25 kDa has become the most commonly used due to its high transfection. Its success has also been attributed to its buffer capacity which endows the polymer with a unique feature of "endosomal escape" that allows to protect therapeutic genes in acidic environment of endosomes and also helps to release the genes in cytosol through endosomolysis (1).

PEI condenses siRNA, forming positively charged polyplexes as described earlier. The net positive charge of polyplexes also leads to interaction with negatively charged cell membrane aiding the cellular uptake and better transfection level (2). However, the same also extrapolates to their higher toxicity as compared to lipofectamine and other cationic phospholipids based formulations. Apart from PEI properties i.e. molecular weight, degree of branching, etc., the efficiency of transfection also varies with polyplex properties i.e. N/P ratio (ratio of nitrogen of PEI to phosphate of DNA), concentration of siRNA, size and zeta potential (3).

Lipofectamine2000 (L2K) is a commercially available cationic lipid widely used due to its effectiveness in producing high transfection efficiencies in certain cell lines when optimized (4). Optimization of such lipid based formulations involves fine-tuning of ratio of cationic lipids to siRNA, siRNA concentration and delivery volume, all of which affect the size, charge and stability of lipoplexes. Such lipoplex formulations have been shown to be more efficient in siRNA delivery than polyplexes and hence, are used in several clinical trials going on for treatment of cancer (5). However, these systems are not devoid of drawbacks which include impaired physicochemical properties *in vivo* due to presence of salts and other molecules. These changes may cause aggregation of complex, dissociation of complex resulting in decreased bioavailability of therapeutic genes and also changes in cellular uptake and transfection efficiency (6). Hence, strategic development of lipoplexes in order to obtain and maintain optimal properties to overcome the barriers to enhance cellular uptake and

transfection needs to be done. In this thesis, Work has been carried out to develop lipoplexes and polyplexes of FGF-2 siRNA.

5.1 Methods

5.1.1 Preparation of siRNA Nanoplexes

5.1.1.1 Preparation of Polyplexes

Polyplex formulations were prepared by incubating polymer solution with siRNA for specific period of time to allow for the ionic reaction between the cationic amino groups of polymer and anionic phosphate groups of siRNA. Precise mixing order of the transfecting solutions is a critical parameter in the outcome of the transfections and therefore the ensuing protocol was followed exactly for all the polymers for the preparation of formulation. Nuclease free water was taken in a 0.5 ml eppendorf tube to make up the final volume of batch to 10 µL. Then, required amount of polymer stock solution was added to prepare the required dilution of polymer. The mixture was then vortexed for 10 min and then, 100 pmole of siRNA was incubated with it for 30 mins at 37°C. Various w/w ratios of polymer/siRNA ranging from 0.5, 1, 1.5, 2, 2.5, 3 and 4 were used to optimize the polyplexes of different modified polymers.

5.1.1.2 Preparation of Lipoplexes

Lipoplexes were prepared by incubating siRNA with preformed liposomes. Briefly, liposomes were prepared by thin film hydration method. Preparation of lipoplexes was carried out based on our previous experience with liposomes and considering basic formulation strategy to produce stable lipoplex formulation that is possible only with the use of stable lipid bilayer forming lipids and Cholesterol. DPPC was used to produce stable lipid bilayer. This lipoplexes were formulated to pulmonary delivery of siRNA which can be tested to compare with polyplex based formulations and carry out *in vitro* cell line studies and *in vivo* studies. In brief, combinations of lipids viz. DOTAP, DOPE, DPPC, Cholesterol, mPEG2000-DSPE in mole ratio of 0.81:0.76:4.84:3.07:0.5 were dissolved in 5 ml of chloroform and methanol mixture (4:1) in a 50 ml round bottom flask and organic solvent was evaporated under vacuum (600 mmHg) and temperature (45°C) using rotary evaporator. The thin lipid film was hydrated by 5 ml of DEPC treated nuclease free water at 60°C. The size of liposomes was reduced using successive extrusion through 1, 0.4, 0.2 and 0.1 µm

polycarbonate membranes using high-pressure extruder. siRNA was incubated with these preformed liposomes at different N/P ratios ranging from 0 to 2.0, for half an hour at 37ºC to get the stable siRNA lipoplexes (DL).

5.1.2 Complexation Efficiency

5.1.2.1 Gel Retardation Assay

Following incubation period, siRNA nanoplexes (polyplexes and lipoplex) were subjected to gel electrophoresis to assess complexation of siRNA. siRNA nanoplexes were mixed with 2 µL of 6X DNA gel loading buffer (Fermentas Life Sciences, USA) and loaded onto a 2% agarose gel containing 0.5 µg/mL ethidium bromide, and electrophoresed for 20 min at 100 V in TBE buffer (10.8 g/L Tris base, 5.5 g/L boric acid and 0.58 g/L EDTA). Afterwards, siRNA was visualized by UV trans-illumination and gel photography using a Gel Doc System (Bio-Rad Lab., USA). Polymer to siRNA w/w ratio and lipid to siRNA N/P ratio were found out by gel electrophoresis for complete complexation of siRNA with polymers/lipid.

5.1.2.2 Centrifugation

Complete complexation assessed by the gel electrophoresis was further confirmed and quantified using centrifugation-UV spectrophotometric analysis. siRNA polyplex were centrifuged at 25,000 rpm for 45 min at 4°C while siRNA lipoplex were centrifuged at 50,000 rpm for 4 hr at 4°C. From these centrifuged samples, aqueous layer was separated out and quantified for siRNA content using NanoDrop UV spectrophotometer.

5.1.3 Determination of siRNA Integrity

The siRNA content in developed nanoplexes was determined to confirm the integrity of siRNA. Polyanion displacement method was used to displace the complexed siRNA from polyplexes and phenol chloroform method was used to extract the siRNA from lipoplexes.

Heparin sodium was used in polyanion competition assay as described in various reports (7-9). In brief, 1 mg/mL of heparin sodium was added to the polyplex formulation equivalent to 100 pmole siRNA and incubated for 20 min. After incubation, the content was analysed by gel electrophoresis method as described in Chapter 3.

In phenol/chloroform extraction method, formulation and phenol-chloroform (1:1 ratio) were mixed in 1:1 volume/volume ratio and then vortexed for 10 min. This emulsion

was then centrifuged at 12,000 rpm at 4°C to separate chloroform and water layer with intermediate phenol layer. Aqueous portion was separated out and analysed by Gel electrophoresis method as described in earlier Chapter 3.

5.1.4 Particle Size and Zeta Potential

The average particle size and zeta potential of siRNA nanoplexes were determined by dynamic light scattering with a Malvern Zetasizer Nano ZS. Prior to the measurement, siRNA nanoplexes were diluted appropriately with nuclease free water and measurements were carried out at 25°C. Zeta potential calculation was performed by Zeta Sizer software using Smoluchowski's equation from the electrophoretic mobility. Each sample was measured three times and the mean values were calculated.

5.1.5 Cell-line Studies

In vitro cell line studies were carried out for further screening of prepared delivery vectors to achieve maximum intracellular siRNA uptake with desired transfection and minimal toxicity. Pulmonary arterial endothelial cell (CPA-47) line was used for all the studies.

5.1.5.1 Sub Culturing Protocol for CPA-47 Cell Line

The CPA-47 cell line was procured from National Culture Collection Society (NCCS), Pune. The cells were maintained as monolayer culture in T-25 cell culture flasks, and medium was replaced two times in a week. Cell were subcultured at 37°C in a humidified atmosphere (95% air and 5% CO_2) using Ham's F12K medium supplemented with penicillin (100 units/ml), streptomycin (100 µg/ml), and 10% horse serum. Below mentioned procedure was followed for the subculturing.

1. Culture medium from the cell culture flask was removed.
2. Trypsin-EDTA solution (2 ml) was added to flask and was shaken to allow the detachment of the cells.
3. Cells were observed under the inverted microscope until cell layer was dispersed (usually within 5 min).
4. Complete medium (2 ml) was added to cell dispersion to neutralise trypsin and then centrifuged at 2000 rpm for 3 min.
5. Pellet of cells was resuspended in minimum volume of complete growth medium.

6. Cell culture was (10^5 Cells) then added to cell culture flask and 10 ml of complete growth medium was added to it.
7. Culture was incubated at 37 °C, 5% CO_2.

5.1.5.2 Cell Counting Using Haemocytometer

A. Preparing Haemocytometer

1. Haemocytometer was cleaned using 70% ethanol.
2. Shoulder of haemocytometer was moistened and a coverslip was affixed using gentle pressure. Newton's ring formation was observed indicating correctly affixed coverslip which ensures correct depth of the chamber.

B. Preparing Cell Suspension

1. Cells were detached from cell culture flask as mentioned above and then suspended in small volume of medium
2. Homogeneous cell suspension was prepared by gentle shaking.
3. Prepared suspension was mixed with equal volume of trypan blue.

C. Counting

1. Small quantity of cell suspension with trypan blue was carefully filled in the haemocytometer chamber using a micropipette by gently placing tip at the edge of the chamber avoiding overfilling of the chamber. Sample drew out of the pipette through capillary action. Pipette was reloaded and second chamber was filled if required.
2. Focus was set on the 16 corner squares of the haemocytometer (as indicated by a circle in the **Figure 5.1** below) using 10X objective of the microscope.

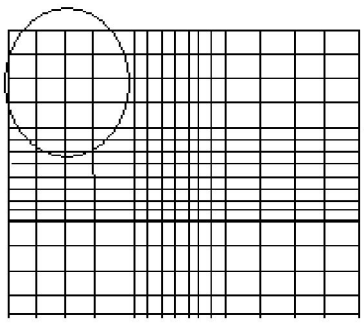

Figure 5.1 Haemocytometer diagram for cellcounting.

3. Number of cells in the 16 square area of haemocytometer was counted using a hand tally counter. Dead cells stained blue by trypan blue were excluded from counting. All live cells within the area and those positioned on the right and bottom edge of 16 squares outer grid were counted while those on left and upper edge (outer edge of haemocytometer chamber) were excluded.
4. Viable cell count was performed on the on all 4 sets of 16 squares at each corner of haemocytometer.
5. Number of cells in one set of 16 corner squares is equivalent to the number of cells in that set x 10^4 /mL.
6. Average number of cells in all 4 sets of 16-square corners was calculated using following equation.

The total count from 4 sets of 16 corners = Average no. of cells/mL x 10^4 x 2

Where 10^4 is conversion factor (conversion of 0.1 mm^3 to ml) and 2 is dilution factor.

5.1.5.3 In Vitro Cytotoxicity Assay

Cell viability and cytotoxicity assays are used for drug screening and estimation of cytotoxicity of chemicals. **Figure 5.2** represents various reagents used for cell viability detection. They are based on various cell functions such as enzyme activity, cell membrane permeability, cell adherence, ATP production, co-enzyme production, and nucleotide uptake activity. Many have established methods such as colony formation method, Crystal Violet method, Tritium-Labeled Thymidine Uptake method, 3-(4,5-dimethylthiazol-2-yl)-2,5-diphenyltetrazolium bromide (MTT), and 4-[3-(4-iodophenyl)-2-(4-nitrophenyl)-2H-5-tetrazolio]-1,3-benzene disulfonate (WST) methods, which are used for counting the number of live cells.

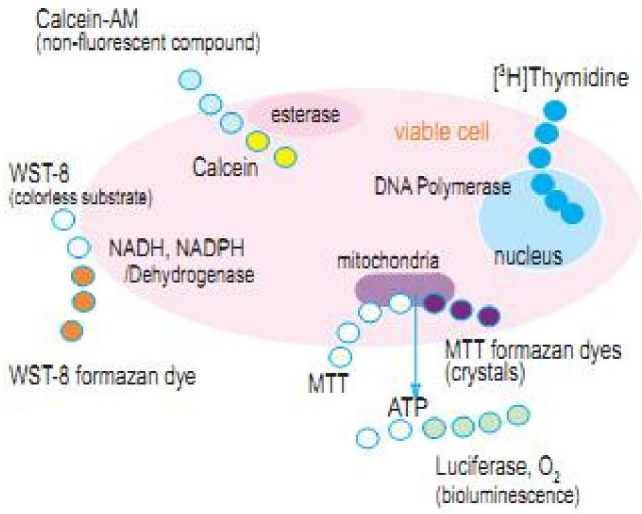

Figure 5.2 Reagents for cell viability assessment.

Enzyme-based methods using MTT and WST rely on a reductive colouring reagent and dehydrogenase in a viable cell to determine cell viability with a colorimetric method. This method is far superior to the previously mentioned methods because it is easy-to-use, safe, reproducible, and is widely used in both cell viability and cytotoxicity tests. Among the enzyme-based assays, the MTT assay is the best known method for determining mitochondrial dehydrogenase activities in the living cells. In the method, MTT is reduced to a purple formazan by hydrogenated nicotinamide adenine dinucleotide (NADH). MTT assay involves the conversion of the water-soluble yellow dye MTT [3-(4,5-dimethylthiazol-2-yl)-2,5-diphenyltetrazolium bromide] to an insoluble purple formazan by the action of mitochondrial reductase. Formazan is then solubilized and its concentration determined by optical densitometry at 570 nm. The result is a sensitive assay with excellent linearity up to 10^6 cells per well.

Protocol: 3-(4, 5-dimethylthiazole-2-yl)-2, 5-di-phenyl tetrazolium bromide (MTT; Himedia, India) assay was used for determination of cytotoxicity of various nanoplexes. CPA-47 cells were seeded onto a 96-well plate at a cell density of 5000 cells/well and allowed to grow in Ham's F12K medium containing 1% antibiotics and 10% horse serum in humidified air at 5% CO_2 concentration for 24 hr. After 24 hr of incubation, cells were separately treated in triplicate with developed polyplexes and lipoplexes formulations i.e. AAP, BAP, CAP, AHP, BHP, CHP, ALP, BLP, CLP, DL and lipoplexes of L2K (L2KL). In case of polyplexes, cytotoxicity was checked at w/w ratios ranging from 1 to 5, while in case of DL, w/w ratio in the range of 4 to 20 was evaluated for 6 hr in Ham's F12 K medium. Then, the transfecting

medium was replaced with complete medium (Ham's F12K medium containing 10% horse serum and 1% antibiotics). The cells were incubated for 48 hr and then treated with 20 µL of 5 mg/mL solution of MTT. After 4 hr of incubation with MTT solution, the culture medium was removed and 200 µL of dimethyl sulfoxide (DMSO) was added and solubilized formazan dye dissolved in DMSO was measured by colorimetry at 570 nm using an Enzyme-Linked ImmunoSorbent Assay (ELISA) plate reader. Cell viability of each treated group (**Table 5.1**) was expressed as a relative percentage against that of negative control, PBS treated cells. Lipoplex formulation of commercially available cationic lipid vector, L2KL, was used as positive control. To assess the toxicity of developed carriers, scrambled sequence of siRNA (negative control siRNA) was used to exclude the interference of therapeutic siRNA on viability of cells.

Table 5.1 Cell line treatment parameters for MTT assay

Sr No	Formulations	Cells	Treatment	Incubation
1.	PP	CPA-47	100 nM NC siRNA	48 hr at 37°C±2 °C and 5% CO_2
2.	AAP		100 nM NC siRNA	
3.	BAP		100 nM NC siRNA	
4.	CAP		100 nM NC siRNA	
5.	AHP		100 nM NC siRNA	
6.	BHP		100 nM NC siRNA	
7.	CHP		100 nM NC siRNA	
8.	ALP		100 nM NC siRNA	
9.	BLP		100 nM NC siRNA	
10.	CLP		100 nM NC siRNA	
11.	DL		100 nM NC siRNA	
12.	PBS*		-	
13.	L2KL*		100 nM NC siRNA	

*Negative control = PBS, Positive control = L2KL

5.1.5.4 In vitro Cell Uptake Studies

For cellular uptake studies, FAM labelled negative control siRNA (FAM-NC-siRNA) was used. Confocal microscopy was utilized for qualitative intracellular accumulation while quantitative cell uptake in terms of mean fluorescent intensity was determined by flow cytometry.

I. Confocal Microscopy

Confocal microscope, in contrast to a conventional microscope, makes use of confocal pinholes that allow light coming only from the plane of focus to reach the detector and hence this excludes the 'out of focus' light coming to the detector. This produces images of exceptional resolution and clarity. This also allows user to collect optical slices of the object for creating three dimensional representation of the sample.

Confocal microscopy provides several advantages over conventional microscopy. These include, firstly, high resolution imaging that allows up to 1.4 times higher resolution than conventional microscopy. High level of sensitivity of confocal microscopy due to highly sensitive detectors and ability to accumulate images captured over time provide better image quality. And as described earlier, if user wishes to perform three dimensional imaging, confocal microscopy makes it possible. Confocal microscopy, also being less invasive form of imaging due to high-power laser illumination and the reduction in light-scattering artifacts, allows non-invasive imaging of thick tissue samples.

In cell biology, confocal microscopy has been utilized for intracellular organelles illumination, cellular uptake determination, intracellular localization of drugs/drug delivery systems etc. This makes it possible to utilize confocal microscopy for cellular uptake studies by using appropriate fluorescent dyes.

Protocol: Cells were seeded at a density of 10^4 cells/well on flame sterilized 0.17 mm square glass cover slips in 6 well plates. After 24 hr of seeding, cells were transfected with naked FAM labelled negative control siRNA (FAM-NC-siRNA) or formulation containing FAM-NC-siRNA (**Table 5.2**) at siRNA concentration of 100 nM. After 6 hr of incubation, cells were washed with cold PBS and immediately fixed using ice cooled 4% paraformaldehyde solution for 10 min. Cells were stained by cell nuclei stain, 4',6-diamidino-2-phenylindole-DAPI, for next 10 min. Cover slips were mounted on slides after three washing with PBS and confocal microscopy was performed using confocal laser scanning microscope.

Table 5.2 Cell line treatment parameters for confocal microscopy and flow-cytometry

Sr No	Formulations	Cells	Treatment	Condition
1	PP	CPA-47	100 nM FAM-NC siRNA	Incubation for 6 h at 37°C And 5% CO_2
2	AAP		100 nM FAM-NC siRNA	
3	BAP		100 nM FAM-NC siRNA	
4	CAP		100 nM FAM-NC siRNA	
5	AHP		100 nM FAM-NC siRNA	
6	BHP		100 nM FAM-NC siRNA	
7	CHP		100 nM FAM-NC siRNA	
8	ALP		100 nM FAM-NC siRNA	
9	BLP		100 nM FAM-NC siRNA	
10	CLP		100 nM FAM-NC siRNA	
11	DL		100 nM FAM-NC siRNA	
12	Naked siRNA		100 nM FAM-NC siRNA	
13	L2KL		100 nM FAM-NC siRNA	

II. Flow Cytometry

Flow cytometry is a technique used in biology to count and examine microscopic particles such as cells, chromosomes etc. The method is used in a number of research and clinical applications like diagnosis of health disorders like cancers, cellular uptake studies of various nanocarriers, and many other applications like molecular biology, pathology, immunology etc. In principle, it involves passage of suspended particles in a fluid stream through an electronic detection system. The particles are sorted on the basis their properties such that to purify the particles of interest. In the field of medicine, it has found its applications in transplantation, haematology, tumor immunology, chemotherapy as well as genetics. So called, Fluorescence Activated Cell Sorting (FACS), is a flow cytometry technique used that makes use of fluorescence for sorting of particles. Fluorescent compound absorbs a higher energy electromagnetic radiation which causes excitation of its electrons to higher energy levels. Electrons, so shifted to higher energy states, decays their energy and reaches ground energy level simultaneously causing emission of low energy electromagnetic radiation, usually of visible range. This so called fluoresced light is quantified using a sensitive high accuracy detector. Among several fluorescent dyes used in FACS, fluorescein isothiocyanate (FITC) is one of the most used dyes. FITC absorbs at its absorption maxima of 488 nm,

resulting in highest emission of 530 nm radiation. One can also make use of other fluorescent dyes that can emit at wavelength other than 530 nm i.e. phycoerythrin that emits at 570 nm when excited at 488 nm.

FACS can be used with nearly any staining procedure, assay or biotechnological process. When fluorescence is introduced in a cell or a formulation through the use of certain fluorescent dyes or therapeutic or diagnostic compounds labeled with such dyes, it can be exploited in flow cytometry for assessing information relating to that specimen (10). By combining the fluidics and laser triggered fluorescence, FACS has become an ideal tool for detection of fluorescently labeled nanoparticles in cells. This gives a quantitative estimation of particles particulate uptake efficiency.

Protocol: CPA-47 cells were seeded in 6-well plates at a density of 5×10^5 cells/well. 24 hr after seeding, cells were exposed to naked FAM-NC-siRNA or formulations (Table 5.2) containing FAM-NC-siRNA at an siRNA concentration of 100 nM and incubated for additional 6 hr at 37°C in humidified air with 5% CO_2. After incubation, cells were washed three times with cold pH 7.4 PBS and then analysed for mean fluorescence activity using fluorescence activated cell sorter. Naked FAM-NC-siRNA and L2KL were used as negative and positive controls, respectively.

5.1.5.5 *In Vitro* Gene Expression Studies by Real Time PCR

Initially, most real-time polymerase chain reaction (RT-PCR) studies targeted a single gene of interest, whose expression reflects the state of disease, response to a drug or a change in the environment and the like. However, most biological phenomena are complex and cannot be described by the expression of individual genes. Instead expression profiles must be measured and interpreted. Traditionally this has been done using microarray techniques, but the development of high throughput platforms opened up the possibility of using the more sensitive and cost efficient real-time PCR technology.

In gene expression profiling, the expression of many genes is measured in many samples. The genes are selected based on the prior knowledge about their function (and often exploratory microarray studies) to be informative in respect to the studied condition. The data are then analysed to identify genes or samples with similar expressions. Reverse transcription combined with the RT-PCR has proven to be a powerful method to quantify gene expression. RT-PCR technology has been adapted to perform quantitative RT-PCR. Two different

methods of analyzing data from real-time, quantitative PCR experiments exist: absolute quantification and relative quantification. Absolute quantification determines the input copy number of the transcript of interest, by relating the PCR signal to a standard curve. Relative quantification describes the change in expression of the target gene relative to some reference group such as an untreated control or a sample at time zero time-course study. Absolute quantification has been combined with real-time PCR and numerous reports have appeared in the literature. In some situations, it may be unnecessary to determine the absolute transcript copy number and reporting the relative change in gene expression will suffice. For example, stating that a given treatment increased the expression of gene x by 2.5-fold may be more relevant than stating that the treatment increased the expression of gene x from 1000 copies to 2500 copies per cell.

Protocol: In vitro mRNA knockdown efficiency of different siRNA formulations was evaluated in order to quantify gene silencing potential of siRNA. RT-PCR was used to quantify the mRNA expressed in CPA-47 cells transfected with different siRNA formulations. CPA-47 cells seeded on a 24 well plate at a density of 10^5 cells/well were incubated for 24 hr to get approximately 80% confluency. After incubation, cells were treated with FGF2 siRNA nanoplex formulations at three different concentrations of siRNA i.e. 25 nM, 50 nM and 75 nM. Cells transfected with L2KL were used as positive control according to manufacturer's protocol. Basal gene expression level was evaluated using PBS control i.e. incubation with phosphate buffer saline. After incubation for 48 hr, total RNA was isolated using TRIzol reagent and reverse transcription into cDNA was carried out using RNA to cDNA conversion kit. mRNA level was quantified using Step One real time PCR using SYBR Green Master mix, forward and reverse primers and 2 ng of cDNA in a total volume of 20 μL. The mRNA expression level of FGF2 gene was normalized against housekeeping gene glyceraldehyde-3-phosphate dehydrogenase (GAPDH). The reaction protocol and specification followed are described below:

I. Selection of Primers

- Primers were selected from primer design tool; NCBI (National Center for Biotechnology Information) (**Table 5.3**).
- The primers for rat FGF2 siRNA were 5′-GTTGCTTCATTTGAAGAGGCTT-3′ for forward and 5′-GTACATGTAGATTAATGTGTGCCA-3′ for reverse (PCR product 148 bp).

- Primers for housekeeping gene GAPDH were 5′-TTATGACCACTGTCCACGCC-3′ for forward and 5′- GGCAGGTCAGATCCACAACA-3′ for reverse (PCR product 222 bp).

II. Total RNA Isolation

1. Equal amount of TRIzol reagent (1 mL/10cm^2) was added to each well and incubated at room temperature for 5 min.

2. Each sample was then transferred to a 2 mL centrifuge tube and 0.2 mL of chloroform was added for every 1mL of TRIzol used. Samples were shaken vigorously for 15 sec and incubated at room temperature for 2-3 min.

3. After incubation, samples were centrifuged for 15 min at 12,000 x g at 4°C.

4. The aqueous phase was transferred to fresh tubes. The aqueous phase was the colourless upper phase that corresponds to ~60% of the volume of TRIzol used. (The interphase was fairly well-defined.)

5. To each separated aqueous phase 0.5 mL of isopropanol for every 1 mL of TRIzol used, was added to precipitate the RNA. Sample was further incubated at room temperature for 10 min.

6. Incubated samples were centrifuged for 10 min at 12,000 x g at 4°C. Pelleted RNA was visible on the side of the tubes.

7. Pellet of RNA obtained after discarding supernatant was washed with 1 mL of 75% ethanol for every 1 mL of TRIzol reagent used. For washing, sampled were mixed by flicking and inverting tubes or by vortexing and further centrifuged at 7500 x g for 5 min at 4°C.

8. Washed RNA pellet was resolubilized in 40 µL of DEPC treated nuclease free deionized water.

Table 5.3 Details of primers

Primer	Sequence (5'->3')	Template strand	Length	Start	Stop	Tm
Bovine FGF2 primers						
Forward primer	GTTGCTTCATTTGAAGAGGCTT	Plus	22	850	871	56.5
Reverse primer	GTACATGTAGATTAATGTGTGCCA	Minus	24	997	974	57.6
GAPDH primers						
Forward primer	TTATGACCACTGTCCACGCC	Plus	20	485	504	60.04
Reverse primer	GGCAGGTCAGATCCACAACA	Minus	20	706	687	59.96

III. RNA to cDNA Conversion

- High capacity RNA-to-cDNA Conversion Kit was utilized to convert RNA into cDNA.
- Kit components were allowed to thaw on ice.
- 1.5 microgram of RNA was used per 20 µL of reaction.
- The Reaction was set up as given below (**Table 5.4**).

Table 5.4 RNA to cDNA conversion parameters

Component	Volume/ Reaction (µL)
2✕ RT (reverse transcription) Buffer	10
20✕ RT (reverse transcription) Enzyme	1
Sample	9

- 20 µL of RT (reverse transcription) reaction mix was added into each well of 48 well plate for real time PCR reaction.
- Plate was sealed and centrifuged to settle down the contents and to eliminate air bubble. Plate was placed in the sample holder of real time PCR system and ran according to cycle given below (**Table 5.5**).

Table 5.5 Steps of RT- PCR cycle

Parameters	Step 1	Step 2	Step 3
Temperature (°C)	37	95	4
Time (min)	60	5	Storage

IV. mRNA Quantification

cDNA from each sample was utilized for mRNA quantification and gene knock-down was accessed. Reaction was set according to below (**Table 5.6**):

Table 5.6 mRNA quantification – reaction parameters

Component	Volume/ Reaction (µL)
Forward primer	0.5
Reverse primer	0.5
cDNA	0.5
Master Mix	10
Nuclease-free H_2O	q.s. to 20

- 20 µL of RT reaction mix was added into each well of 48 well plate for real time PCR reaction.
- Plate was sealed and centrifuged to settle down the contents and to eliminate air bubble. Plate was placed in the sample holder of real time PCR system and ran according cycle given below (**Table 5.7**).

Table 5.7 RT-PCR cycle steps

Parameters	Step 1	Step 2	No. of cycles
Temperature (°C)	95	60	40
Time (seconds)	15	90	

5.1.5.6 *In Vitro* Cell Line Studies of Optimized Formulation at Low Oxygen Tension

Hypoxia can be defined as low oxygen tension to the organ, tissue or cells either due to reduced oxygen supply or due to increased consumption of oxygen. And hypoxia makes the prime cause of hypertension leading to angiogenesis and proliferation of arterial endothelial cells. By mechanism, endothelial cells sense reduction in oxygen levels through a number of oxygen sensitive transcription factors known as hypoxia induced factors (11). These hypoxia induced factors mainly involve various angiogenic factors and their receptors which show differential expression under normoxic and hypoxic conditions. For example, VEGF and its receptors show increased expression in endothelial cells under hypoxic conditions (12). So is the case with FGF-2 and its receptors (13). Such changes mediate different biological

changes including restructuring of actin filaments, migration in collagen matrix, amplification of angiogenic capabilities, all of which leading to remodelling of capillary network (12).

In order to simulate the *in vivo* conditions of hypoxia, we have used pulmonary arterial endothelial cells grown under hypoxic conditions. Such study will give an exact idea about the cellular uptake, cytotoxicity and gene expression under pathological condition and help correlate the results obtained in normoxic and hypoxic conditions as well as to establish an extrapolation for animal studies.

Protocol: CPA-47 cells were cultured in Ham's F12K medium supplemented with 10% horse serum and 100 units/ml penicillin + 100 μg/ml streptomycin. Cells were grown under normoxic conditions overnight at required cell densities in required well plates for adherence. Cells were exposed to hypoxic environment at 37°C for 24 hrs. A hypoxic environment was created by placing the well plates with one pouch of Anaero Pack into an airtight jar (14, 15).

Cells were grown under hypoxic conditions as described above and different *in vitro* evaluations i.e. cytotoxicity study using MTT assay, qualitative and quantitative cellular uptake studies using confocal microscopy and flow cytometry, respectively and gene expression study using RT-PCR for different nanoplexex were carried out. The protocols followed were as described in previous sections except for the incubation conditions used i.e. hypoxic environment instead of normoxic conditions used.

5.1.6 Heparin Polyanion Competition Assay

Heparin polyanion competition assay was used to assess the stability of developed nanoplexes. *In vivo* efficacy of siRNA complexes is achieved after their successful transfection through negatively charged cell membrane. But, the transfection of siRNA can be limited due to unwanted exchange of siRNA with large polyanions found outside cells such as sulphated glycosaminoglycans (GAGs). Low charge density of complexes may be one of the reasons behind reduced efficacy of siRNA formulations (16). Thus, it can provide a significant impact to estimate the transfection ability of siRNA complexes in vitro through the polyanion competition assay (17).

Interactions between GAGs and developed siRNA delivery system could hinder gene transfer towards the target cell and reduce cellular uptake. Binding of positively charged siRNA complexes with negatively charged GAGs leads to dissociation of siRNA from the

complexes or by changing size and surface charge to cause dissociation of the complexes (18). Heparin and hyaluronic acid (HA) are the GAGs which are present in the extracellular matrix and on the surface of different cell types at different concentrations (19).

Protocol: This assay was used to evaluate the stability of siRNA nanoplexes *in vivo* and to confirm that siRNA forms stable complexes with synthesized polymers and developed liposomes which are resistant to decomplexation by large polyanions like sulphated glycosaminoglycans found inside the body. The formulations equivalents to 1.32 µg of siRNA were then exposed to varying amounts of heparin sodium (0.1 to 0.7 mg/mL). Resulting dispersions were allowed to incubate at room temperature for 15 min. After incubation the amount of siRNA released from different formulations was evaluated using 2% agarose gel electrophoresis (Chapter 3). The gel was analysed by staining with ethidium bromide and observed using GelDoc™ XR^+ Imaging System.

5.1.7 Serum Stability Study

The primary objective of any therapeutic gene delivery system is to deliver gene to the desired site of action in required concentration. But for siRNAs, it is difficult to retain their functional activity, as formulations thereof must resist degradation by various nucleases in circulation prior to cellular internalization. Several studies have concluded that half-life of siRNAs in plasma, when delivered naked, is very low and ranges from several minutes to around an hour (20). This barrier impedes attainment of efficient therapeutic effect on systemic application of naked, unmodified siRNAs. Several novel approaches were invented to overcome this obstacle which includes chemical modifications to the nucleotides (e.g., 2'-F, 2'-OMe, LNA) or the backbone (e.g., phosphorothioate linkages) resulting in enhanced nuclease stability and prolonged siRNA half-life in serum maintaining the siRNA efficacy at target site (21). According to some studies about 70% of the systemically administered siRNA degrades within 1 min resulting in diminished therapeutic response (22). Additionally, carrier systems like lipoplexes and polyplexes have provided improvement in transfection efficiency of siRNAs, as they are protected by the carrier. However, hydrodynamic injection (HDI) is reported to provide efficient transfection of naked siRNAs *in vivo* (23). But with such approach, exposure time of siRNA to the bloodstream prior to cellular uptake by cells such as hepatocytes is not precisely known and even a short exposure is sufficient to degrade a portion of the injected unmodified siRNAs. Thus, approach of carrier system was considered the best approach to deliver siRNAs. However, with carrier systems too, presence

of serum causes unwanted changes that may affect the stability of complexed siRNA. Therefore an *in vitro* assessment of protective effect of carrier system can give idea of their *in vivo* behaviour.

Protocol: This study was performed to estimate stability of complexed siRNA present in nanoplexes in presence of serum, as there is a possibility for *in vivo* degradation during circulation, and degradation due to extracellular and intracellular RNAses. Naked siRNA and different siRNA nanoplex formulations containing 1.32 µg of siRNA were incubated with 10 µL non-heat inactivated FBS at 37°C for various time periods such that final incubation volume had 50% serum concentration. Incubated samples were then analysed for intact siRNA using gel electrophoresis as per the following protocols:

1. Polyplexes were analysed by heparin competition assay. As described in heparin competition assay, 0.5 mg/mL and 0.6 mg/mL heparin was able to completely displace 1.32 µg siRNA from ALP/AAP polyplexes and from AHP polyplexes, respectively. After incubation with serum for specified time, 0.5 M EDTA solution was added to samples (1 µL of EDTA solution for 10 µL of serum used) and gently mixed to inactivate any nuclease activity (24). EDTA treated samples were then treated with heparin at a concentration of 1 mg/mL to ensure complete release of siRNA from polyplexes. Released siRNA was further detected by gel electrophoresis as described in chapter 3. siRNA band density obtained at 0 min time point was considered 100% and % siRNA retained at later time points were calculated relative to the 0 time band density. Any degradation of siRNA would appear as decrease in the band intensity relative to initial.

2. In case of lipoplexes, phenol/chloroform extraction method was used for analyses. Equal volume of phenol/chloroform mixture (1:1 v/v) was added to the samples and then vortexed. The resulting dispersion was then centrifuged at 14,000 rpm for 10 min at 4°C temperature. After centrifugation, aqueous layer was separated and subsequently mixed with loading buffer and was loaded onto 2% agarose gel as previously mentioned (25). The samples were analysed after ethidium bromide staining using GelDoc™ XR$^+$ Imaging System (BioRad, USA).

5.1.8 Salt Induced Aggregation Study

Stability of nanoplexes depends on the electrostatic interaction between the siRNA and cationic polymer or lipid. In contrast to the large polynucleotides like plasmid DNA, in case of short molecules like siRNA, as it depends on the number of charge per molecule, the stability is much influenced by presence of electrolytes. Salts like sodium chloride can disrupt electrostatic interactions causing particle size change through aggregation and then leading to dissociation of polyplexes at certain concentration. Dynamic light scattering can be used for salt induced aggregation as well as dissociation of polyplexes.

The electrolyte induced flocculation test is also used to evaluate the steric stability of PEGylated liposome formulations (26). Competitive forces of attraction (van der Waals forces) and repulsion (either electrostatic repulsive forces or steric stabilizing barrier or both) are mainly responsible for the physical stability of a dispersed system. Additionally, various other interactions (depletion and steric interactions) also show an important role in stability of formulations (27). Non-ionic polymer molecules on particulate surface prevent particles from coming close enough to allow van der Waals attractive forces between the particles to dominate and thus create steric barriers resulting in steric stabilization (28). Electrostatically stabilized conventional liposomes, when exposed to electrolytes, face compression of electrostatic double layer surrounding the liposomes and subsequent aggregation followed by flocculation with increase in optical turbidity (29). But, if the formulations are stabilized by hydrated steric stabilizing barriers, the system would remain stable even if the electrostatic double layers have been compressed.

Protocol: This test was performed to estimate the stability of prepared formulations in presence of electrolytes. siRNA nanoplexes were diluted to obtain 100 nM concentration of siRNA. Particle sizes of all formulations were measured by dynamic light scattering using Malvern Zeta-Sizer. Accurately weighted quantities of sodium chloride were solubilized in a step-wise manner to obtain concentration of 1%, 2%, 3%, 4% and 5% w/v sodium chloride concentration and particle size of each formulation was measured after each addition.

5.1.9 Stability Study in Bronchoalveolar Lavage Fluid

As in case of the polyplexes and lipoplexes to be used for intravenous route where stability in presence of serum becomes important, those to be administered into the lungs through intra-tracheal route of through aerosolization, stability with the extracellular substances present in

the airways fluid becomes of concern. This follows the fact that airway surface fluid contains various surfactants and proteins that might cause instability of siRNA complexes through interaction with various components like mucin, glycoprotein, albumin, surfactants etc. (30). This in turn affects the gene transfection by formulations as it affects the surface properties of gene delivery vectors. Bronchoalveolar lavage (BAL) fluid can be chosen as a model fluid system to simulate the possible interactions of airway surface fluid with polyplexes and lipoplexes. Moreover, such fluids exhibit significant nuclease activity. Hence, siRNA released due to interaction with lavage fluids may get degraded and in order to determine whether pulmonary administration of prepared nanoplexes would affect stability in presence of BAL fluid, this study was performed.

Protocol: Rats were euthanized by an overdose of intraperitoneal injection of pentobartital (75 mg/mL). The trachea was exposed and cannulated with a 20-gauge catheter. After instillation of 1.5 mL of cold sterile PBS three times through the trachea into the lung, BALF was recovered at 50% to 60% of the original volume. The BALF was centrifuged for 10 min at 1500 rpm to separate any debris and cells.

10 µL volumes of formulation containing 1.32 µg of siRNA were prepared in 0.5 mL eppendorff tubes and treated with 10 µL of BALF. Intact siRNA retained in each treated sample was determined at intervals of 15 min over a period of 2 hr using gel electrophoresis as follows.

1. Polyplexes were analysed by heparin competition assay. After incubation with BALF for specified time period, 0.5 M EDTA solution was added to samples (1 µL of EDTA solution for 10 µL of BALF used) and gently mixed to inactivate any nuclease activity (24). EDTA treated samples were then treated with heparin at a concentration of 1 mg/mL to ensure 100% release of siRNA from polyplexes. Released siRNA was further detected by gel electrophoresis as described in chapter 3. siRNA band density obtained at 0 min time point was considered 100% and % siRNA retained at later time points were calculated relative to the 0 time band density.

2. In case of lipoplexes, phenol/chloroform extraction method was used for analyses. 100 µL of phenol/chloroform (1:1 v/v) was added to the samples and then vortexed. The resulting dispersion was then centrifuged at 14,000 rpm for 10 min at 4°C temperature. After centrifugation, 25 µL was withdrawn from the seperated aqueous layer and subsequently mixed with 5 µL loading buffer and was loaded onto 2%

agarose gel (25). The samples were analysed after ethidium bromide staining using GelDoc™ XR^+ Imaging System (BioRad, USA).

5.1.10 Transmission Electron Microscopy

Morphology, lamellarity and vesicle size were studied using Cryo-TEM (TECNAI G2 Spirit Bio TWIN, FEI-Netherlands) operating at 200 kV with resolution of 0.27 nm and magnifications at the order of 750,000X. Hydrophobic carbon grid was converted to hydrophilic nature by using Glow Discharge to perform cryo-TEM. Formulation was evenly spread on prepared grid and the grid was cryo-freezed in liquid ethane at -180°C. Cryo-freezed grid was transferred to cryo-holder maintained at -175°C using liquid nitrogen storage box. The cryo-holder was then inserted in the microscope for imaging the sample. Combination of bright field imaging at increasing magnification and diffraction modes was used to reveal the form, lamellarity and particle size of the prepared formulation.

Morphology and particle size of polyplexes were evaluated using Transmission Electron Microscopy (TEM) on Technai 20 Transmission Electron Microscope. A drop of sample was placed onto a 300 mesh copper grid coated with carbon. Approximately 2 min after deposition, the grid was tapped with filter paper to remove surface water and make it dry. Then it was treated with uranyl acetate for negative staining. After 5 min, the grid was placed in sample probe and inserted in Microscope which was then observed at 200 kV accelerating voltage with suitable magnification between 25x to 75000x.

5.2 Results and Discussion

5.2.1 siRNA Complexation

The conjugation of amino acid residues on the primary amines of PEI might affect the polymer's ability to form a complex with siRNA. For this reason, we examined the influence of the conjugation of amino acids on the formation of polyplexes by using the gel retardation assay. Optimized formulations were further confirmed by NanoDrop UV spectroscopic determination of siRNA complexation efficiency. Charge dependent migration of siRNA towards anode under electric potential in gel retardation assay helps to evaluate the complexation efficiency of nanoplexes. In principle, when siRNA is complexed with cationic lipid/polymer, migration of siRNA is retarded and siRNA remains inside the wells. However, if there is any uncomplexed siRNA, it will migrate on the gel under electromotive force

giving a band visible under UV light. Images (**Figure 5.3, Figure 5.4, Figure 5.5, Figure 5.6** and **Figure 5.7**) captured using Image Lab software on UV gel illuminator have shown the optimized w/w ratios of different polymers-to-siRNA. The data for different ratios for all the polymers have been given in **Table 5.8.** Corresponding N/P ratios were calculated for all w/w ratios used for polyplex preparation (**Table 5.8**) by using amines of polymers and phosphate of siRNA. Obtained molecular weight of polymer and degree of substitution on the polymer were used to find out number of amines involved in the formation of polyplexes.

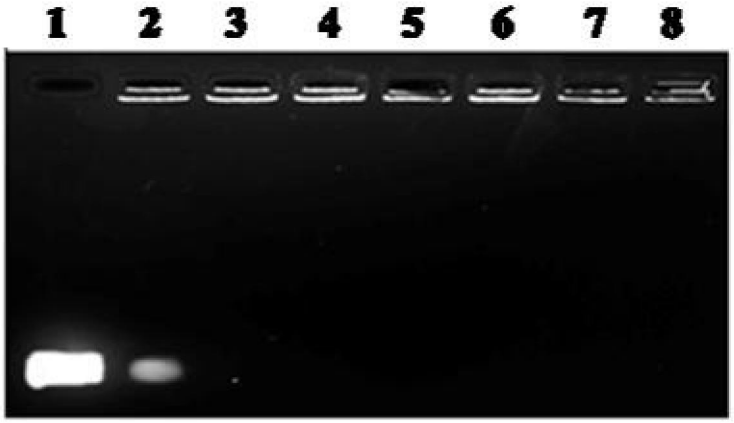

Figure 5.3 Gel retardation assay of PP.

(PEI/siRNA w/w ratio→Lane 1: Naked siRNA; Lane 2: 0.5; Lane 3: 0.75 ; Lane 4: 1 ; Lane 5: 1.5 ; Lane 6: 2 ; Lane 7: 3 ; Lane 8: 4).

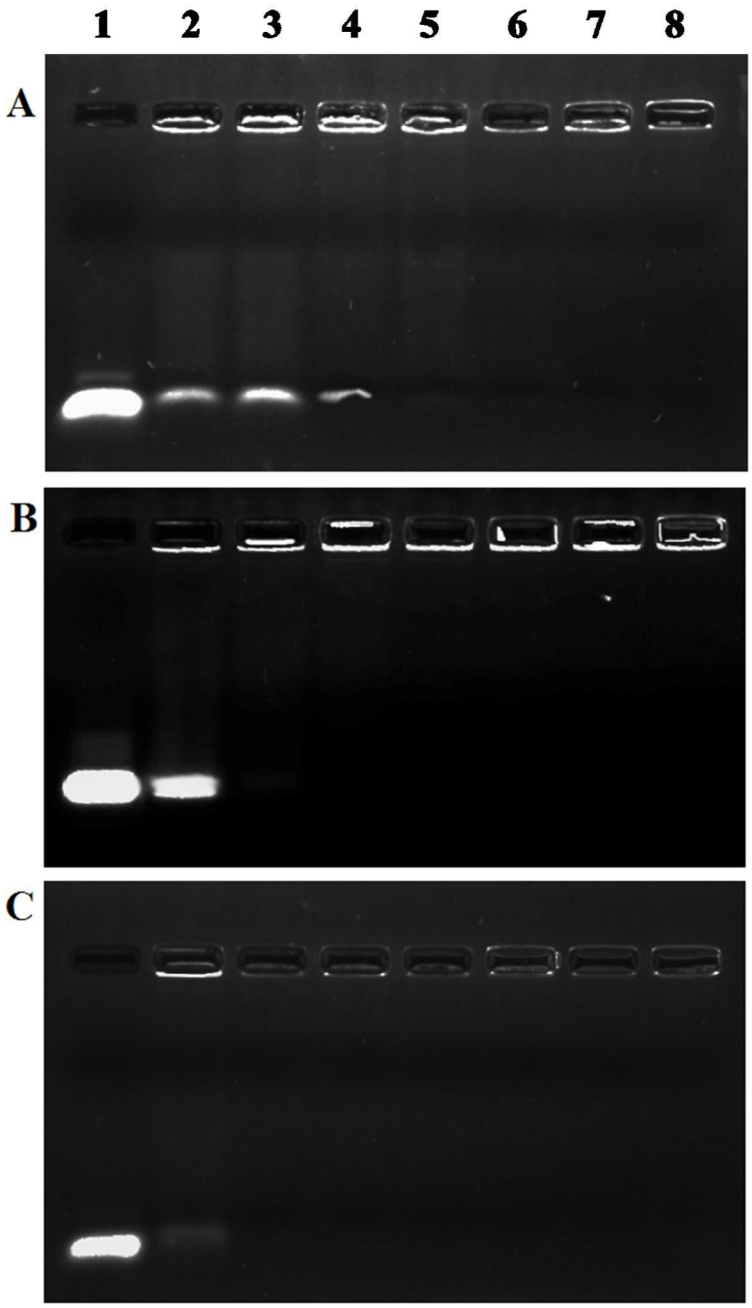

Figure 5.4 Gel retardation assay of (A) ALP, (B) BLP and (C) CLP.
(Polymer:siRNA w/w ratio→ Lane 1: Naked siRNA; Lane 2: 0.5; Lane 3: 1; Lane 4: 1.5 ; Lane 5: 2 ; Lane 6: 2.5 ; Lane 7: 3 ; Lane 8: 4).

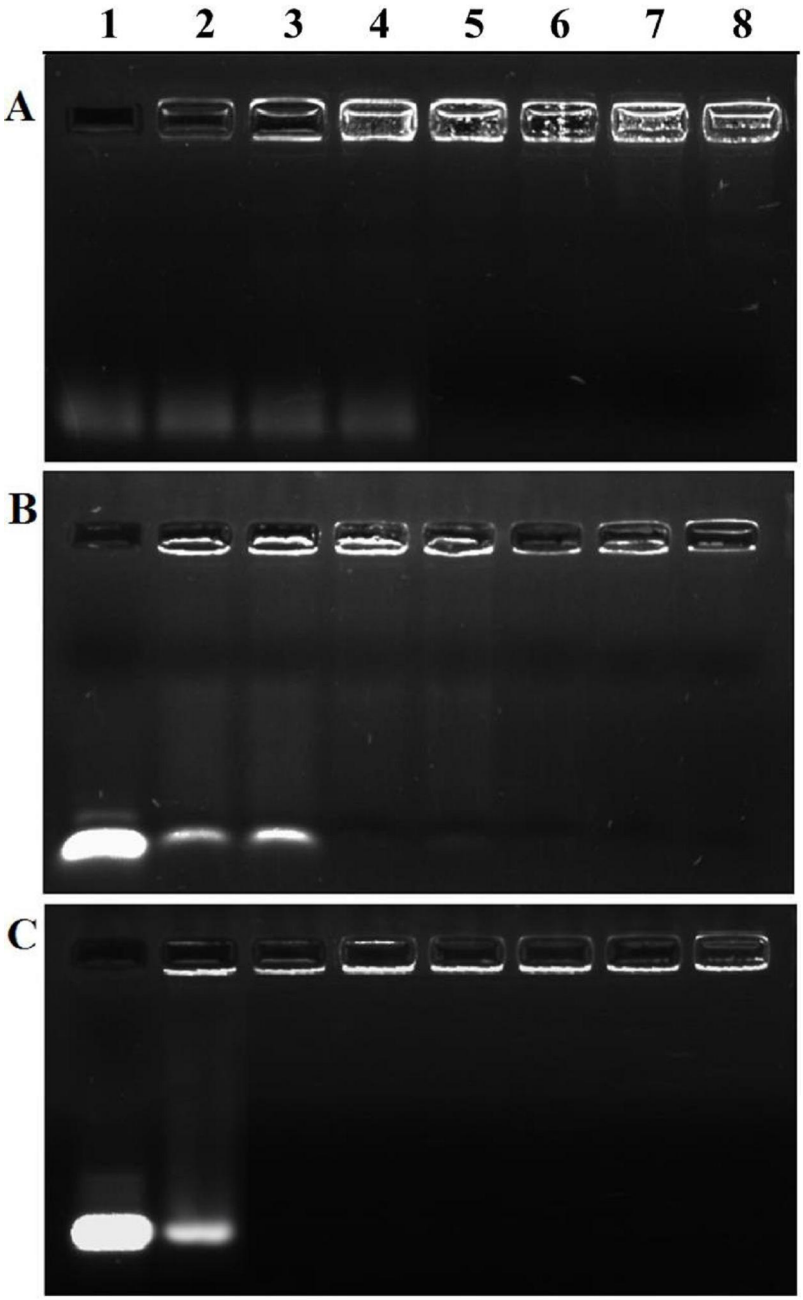

Figure 5.5 Gel retardation assay of (A) AAP, (B) BAP and (C) CAP.
(Polymer:siRNA w/w ratio→ Lane 1: Naked siRNA; Lane 2: 0.5; Lane 3: 1; Lane 4: 1.5 ; Lane 5: 2 ; Lane 6: 2.5 ; Lane 7: 3 ; Lane 8: 4).

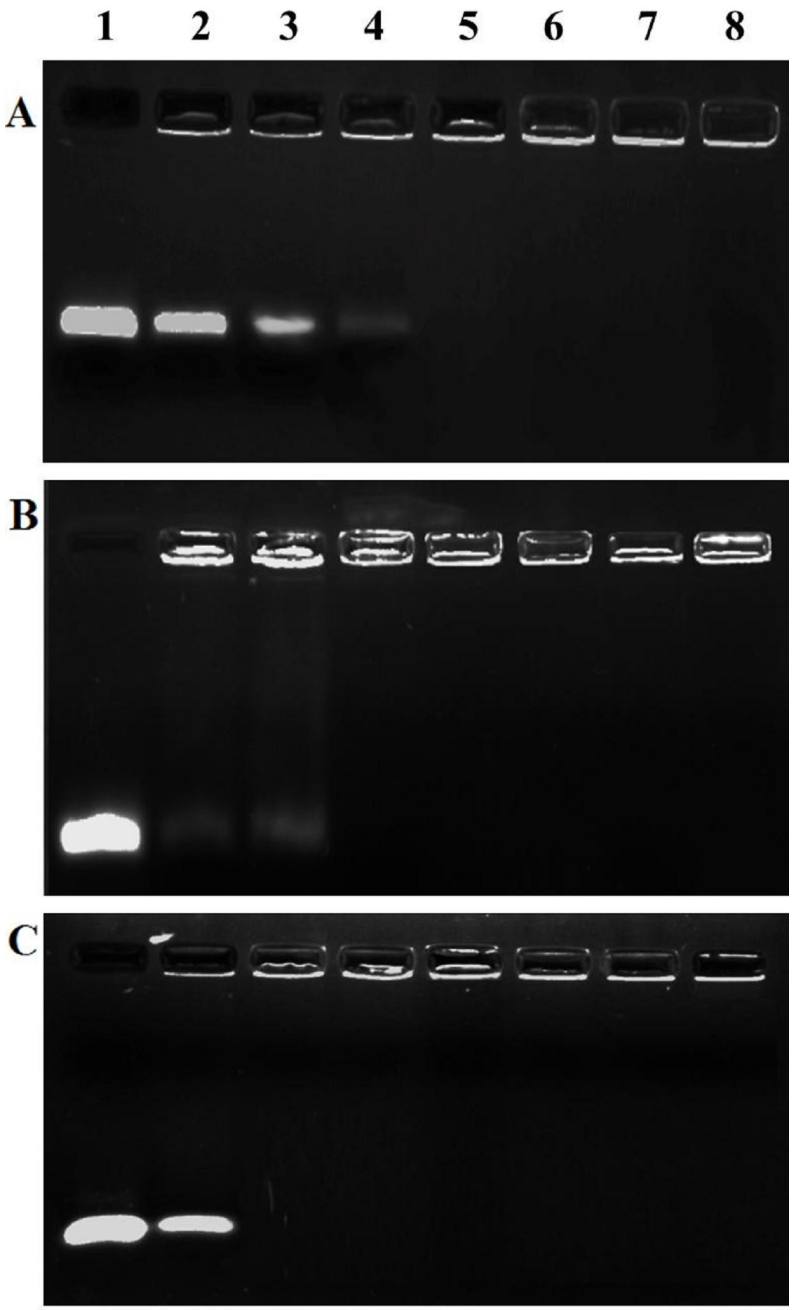

Figure 5.6 Gel retardation assay of (A) AHP, (B) BHP and (C) CHP.
(Polymer:siRNA w/w ratio→ Lane 1: Naked siRNA; Lane 2: 0.5; Lane 3: 1; Lane 4: 1.5 ; Lane 5: 2 ; Lane 6: 2.5 ; Lane 7: 3 ; Lane 8: 4).

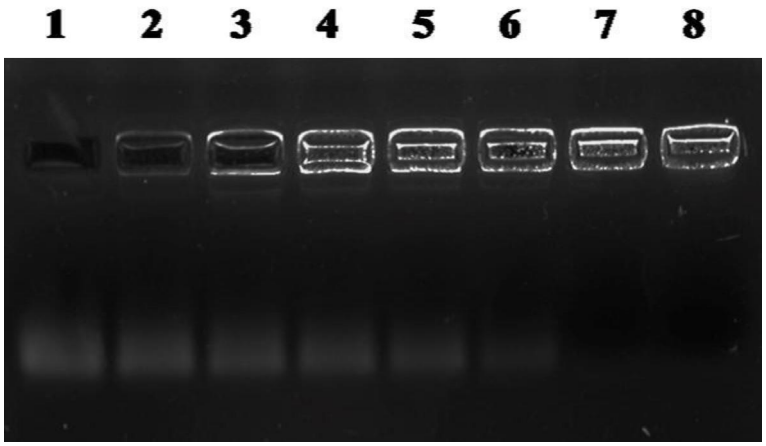

Figure 5.7 Gel retardation assay of DL.

Lipid:siRNA N/P ratio→ (Lane 1: Naked siRNA; Lane 2: 0.25; Lane 3: 0.5; Lane 4: 0.75; Lane 5: 1.0; Lane 6: 1.5; Lane 7: 2.0; Lane 8: 4.0).

Table 5.8 Different optimized siRNA formulations

Sr No	Formulation	Optimized w/w Ratio	Optimized N/P Ratio	*Complexation Efficiency (%)
1.	siRNA-PEI Polyplex (PP)	0.75	6	98.21±1.32
2.	siRNA-AA Polyplex (AAP)	2	12	97.37±1.43
3.	siRNA-BA Polyplex (BAP)	1.5	9.5	96.41±0.97
4.	siRNA-CA Polyplex (CAP)	1	6.5	97.13±2.31
5.	siRNA-AH Polyplex (AHP)	2	13	95.18±1.17
6.	siRNA-BH Polyplex (BHP)	1.5	10	96.21±2.54
7.	siRNA-CH Polyplex (CHP)	1	7	96.94±1.24
8.	siRNA-AL Polyplex (ALP)	2	11.25	98.37±1.09
9.	siRNA-BL Polyplex (BLP)	1.5	9	96.57±1.26
10.	siRNA-CL Polyplex (CLP)	1	6.5	96.17±1.39
11.	siRNA-Liposomes (DL)	4	2	96.64±0.96

*Values are represented as mean±SD, n=3.

All the synthesized polymers were able to condense more than 95% of siRNA at their optimized polymer-to-siRNA weight ratios. Polymer-to-siRNA weight ratios were different for different degree of substitution. Optimized PEI-to-siRNA weight ratio was 0.75 w/w which was equivalent to N/P ratio of 6 (**Table 5.8**) which was in concordance with other

previous reports which proved that PEI/DNA complex at N/P ratio of 6 (31). However, in case of amino acid conjugated PEI, polymer-to-siRNA weight ratios were higher. And as the conjugation level of Boc-amino acid increased, the N/P ratio for complete complexation increased. It is reported that PEI has pKa values of around 10 for primary, and 7.95 for secondary amino groups, thus at physiologic pH only the primary amines are protonated while the secondary amines are partially protonated (32). Since the conjugation occurred at various fractions of primary amino groups of PEI which are actively involved in siRNA complexation in native PEI, conjugated amino groups would subsequently not be available for binding and hence would require to be compensated by increasing w/w and N/P ratio. The presence of bulkier Boc group of Boc-amino acid also masks the ionisable functional groups which can affect the electrostatic interactions. Thus, if the proposed modification affects the amount of ionized groups present on the native polymer at the binding conditions, the N/P ratio along with the w/w ratio required for binding is increased in case of modified polymer to compensate for available ionized groups. **Figure 5.8** and **Figure 5.9** shows that the integrity of siRNA after complexation with polymers/lipids was retained as it was before complexation. When we compared the siRNA with 10 bp ladder, it didn't show any degradation or instability of siRNA incorporated in nanoplex form.

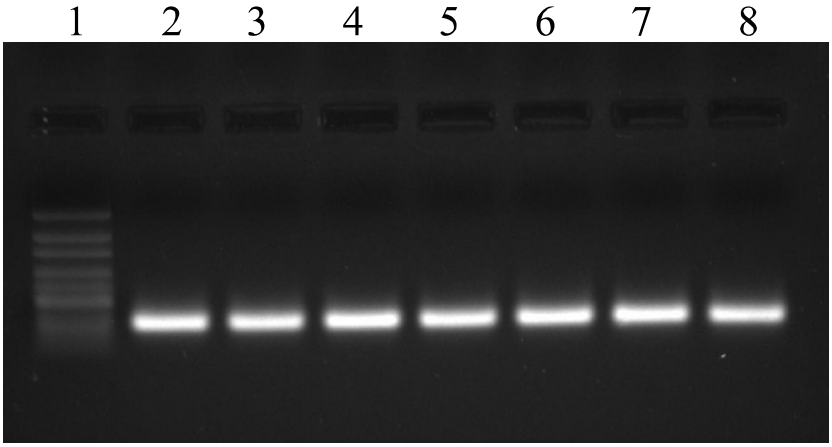

Figure 5.8 Integrity of siRNA after complexation with polymers.
(Lane 1: ladder; Lane 2:PP; Lane 3:CAP; Lane 4:BAP; Lane 5:AAP; Lane 6:CHP; Lane 7:BHP; Lane 8:AHP).

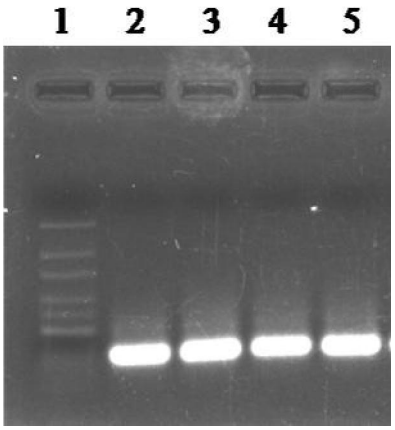

Figure 5.9 Integrity of siRNA after complexation with polymers/lipids.
(Lane 1:ladder; Lane 2:ALP; Lane 3:BLP; Lane 4:CLP; Lane 5:DL).

In development of liposomes, DOTAP and DOPE were used in combination, but due to their low Tg, the prepared formulation was not physic-chemically good enough (33). Further, to impart rigidity and stability to liposomes DPPC and Cholesterol were added. DSPE-mPEG$_{2000}$ was added to liposomes to incorporate the surface shielding effect by PEG chain and to improve the *in vivo* activity of developed liposomes in lung. Further studies were carried out by using the combination of DOTAP, DOPE, DPPC, Cholesterol and DSPE-mPEG$_{2000}$. In case of lipoplexes, optimized N/P ratio was found to be 2. Parker et al. showed that DOTAP for N/P=1.8, equivalent to DOTAP/nucleic acid w/w ratio of 4, had a good complexation efficiency (34). These results demonstrated that the PEI/modified PEIs/lipids were able to complexes siRNA through electrostatic interactions between ionisable amino groups and phosphates of siRNA.

5.2.2 Particle Size and Zeta Potential

The surface charge of a gene delivery vector at physiologic pH is important for its coulumbic interactions with therapeutic genes and later, for the cellular entry of formulation through interaction with the negatively charged cell membrane. PEI retained sufficient positive surface charge even after substitution with different Boc-amino acid moieties, as indicated by zeta potential determinations. At optimized w/w ratio of Boc-amino acid-PEI complexes, a strongly positive zeta potential (about +15 to +35 mV) was formed by excess cations that are not involved in binding with siRNA. The net positive charge remaining on polyplexes formed with modified PEIs would cause electrostatic repulsion between complexes that would

prevent aggregation. This positive charge will also facilitate electrostatic interaction between the polyplexes and the negatively charged surface membranes of cells (35).

Table 5.9 Particle size and zeta potential of nanoplexes

Sr No	Formulation	Particle Size (nm)	Mean PDI	Zeta Potential (mV)
1.	PP	101.2±4.3	0.15	36.87±2.52
2.	AAP	153.9±5.6	0.06	13.97±1.32
3.	BAP	137.5±2.9	0.08	21.10±2.20
4.	CAP	118.0±4.6	0.10	28.53±1.02
5.	AHP	138.2±5.5	0.12	20.73±2.75
6.	BHP	128.7±1.9	0.08	26.80±1.09
7.	CHP	112.4±2.6	0.13	33.27±2.30
8.	ALP	167.9±2.7	0.11	14.17±2.52
9.	BLP	158.1±3.2	0.10	21.33±2.05
10.	CLP	133.1±1.7	0.08	30.73±1.65
11.	DL	120.2±2.5	0.10	28.65±2.0

*Values are represented as mean±SD, n=3.

-

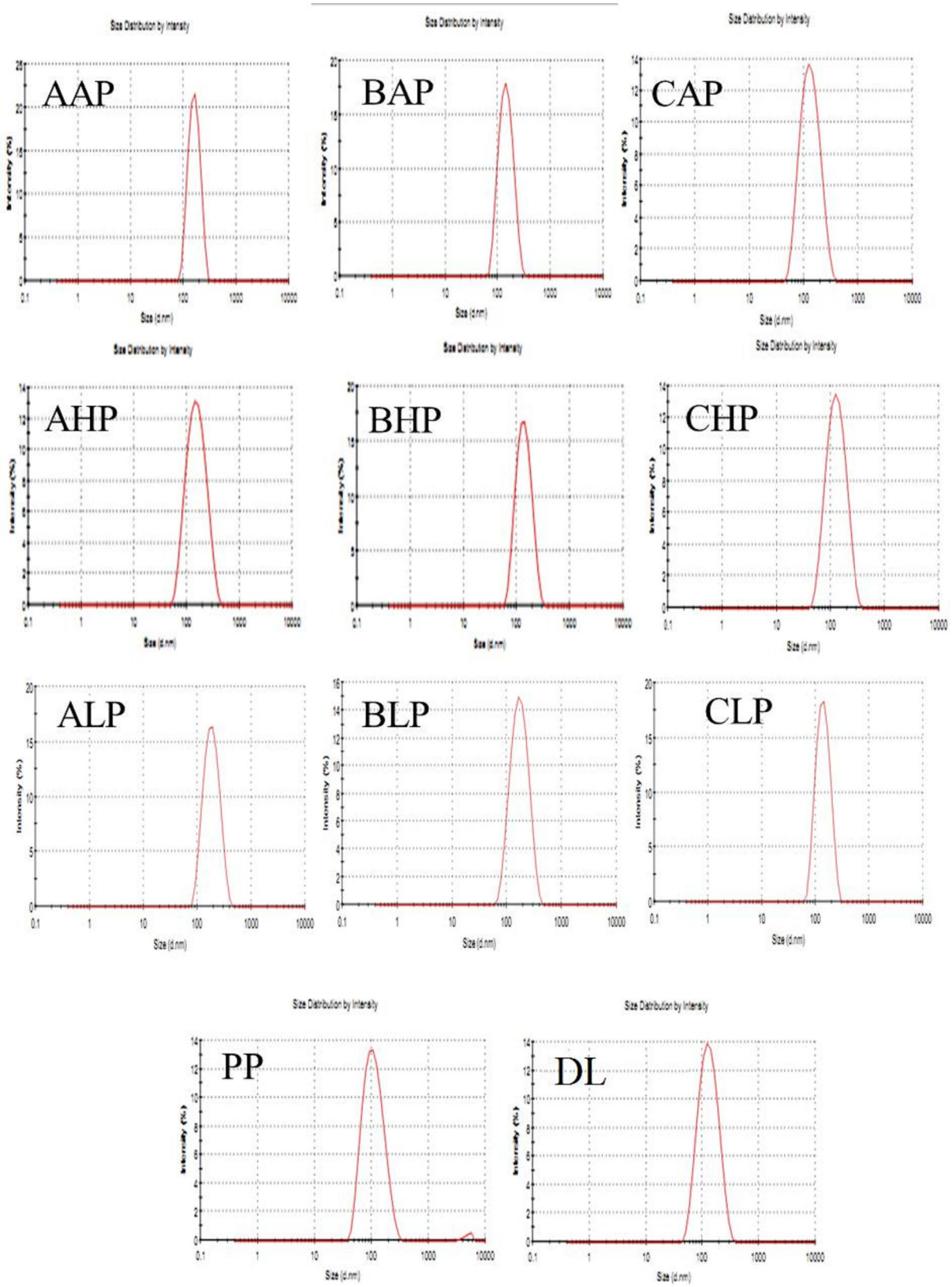

Figure 5.10 Particle sizes of different nanoplexes.

As the degree of substitution increased, the zeta potential decreased concomitantly in all of the three series of Boc-amino acid modified PEIs (**Table 5.9**). The decrease in zeta potential can be explained by the shielding of primary amino functions which act as cationic sites on PEI. However, at each degree of substitution, zeta potential was higher with Boc-histidine modified PEI as compared to other two, Boc-alanine-PEI and Boc-leucine-PEI, which might be attributed to partial ionization of imidazole ring nitrogen which is having pKa of ~7. This compensates, to some extent, for the loss of positive charges conferred on polymer through conjugation. A linear relation between zeta potential and degree of substitution on primary amine of PEI was found.

The particle size measurements indicated that the polyplexes formed from Boc-amino acid derivatives of PEI are larger than those formed from native PEI. As was the case with zeta potential, degree of substitution by Boc-amino acid also affected the particle size. As the substitution level increased, the particle size also increased which can be due to shifted hydrophobicity and charge balance. Substituents are expected to orientate towards the surface of modified polymers leading to shielding of positive charges and hydrophilic elements. Reduced charge of polymer would reduce the capacity of polymer to efficiently compact siRNA (i.e. making loose complexes as compared to native PEI). The increase in hydrodynamic diameters is compatible with the hypothesis that substitution of Boc-amino acid is associated with increased steric hindrance and charge shielding during complex formation. Previous reports showing the effects of different substituents, nature of substituents and degree of conjugation on particle size of PEI polyplexes also support the results (36).

Mean particle size of PP was 101.2 nm with low polydispersity index of 0.15 which suggest uniform particle size distribution within the formulation. However, the charge compensation provided by imidazole ring in case of Boc-histidine made Boc-histidine-PEI show low particle size increase as compared to other Boc-amino acid-PEIs at each conjugation level. And though increased, particle sizes for all the type of polyplexes were less than 170 nm with low polydispersity index (<0.2) (**Figure 5.10**). Our results demonstrated that AAP, BAP, CAP, AHP, BHP, CHP, ALP, BLP and CLP have suitable physicochemical properties for being efficient gene delivery systems.

DL lipoplex formulations showed mean of particle size of 120.2 nm, which was 109.3 nm before siRNA complexation. Increase in size can be attributed to the siRNA adsorption on the surface of preformed cationic liposomes.

5.2.3 In Vitro Cell Cytotoxicity Study

This work reports the effects of different degrees of Boc-amino acid conjugation to PEI on cytotoxicity by using a tetrazolium-based MTT colorimetric assay. Cytotoxicity of cationic polymers is mainly due to their aggregation on cell surfaces, which impairs the important membrane functions of cells (37). Polymers may also interfere with critical intracellular processes of cells; in particular, primary amine has been reported to disrupt Protein Kinase-C function through disturbance of protein kinase activity (37). Moreover, Moghimi et al. have shown that PEI induces two types of cytotoxicity, a necrotic membrane permeabilizing cytotoxic mechanism that begins within 30 min and an apoptotic mechanism that starts at 24 hr. The necrotic cytotoxicity is related to the strong positive charge on PEI, resulting from electrostatic interaction with the negatively-charged cell membrane (38). Zintchenko et al. has reported that reducing the surface charge of PEI is a strategy to decrease PEI cytotoxicity (39).

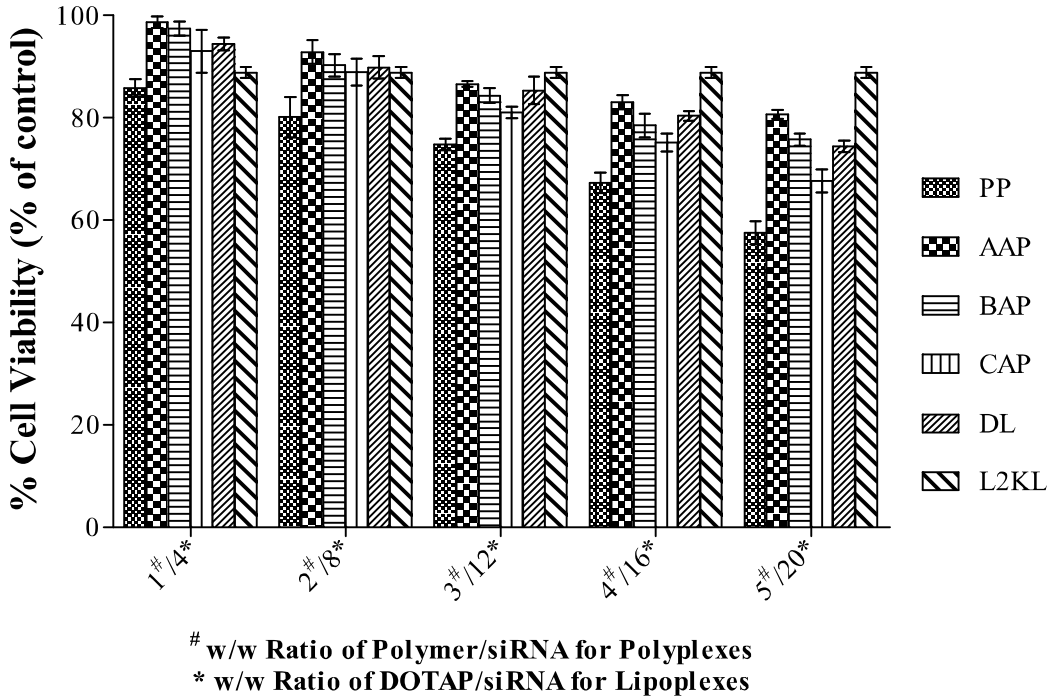

Figure 5.11 Cytotoxicity of AAP, BAP and CAP.

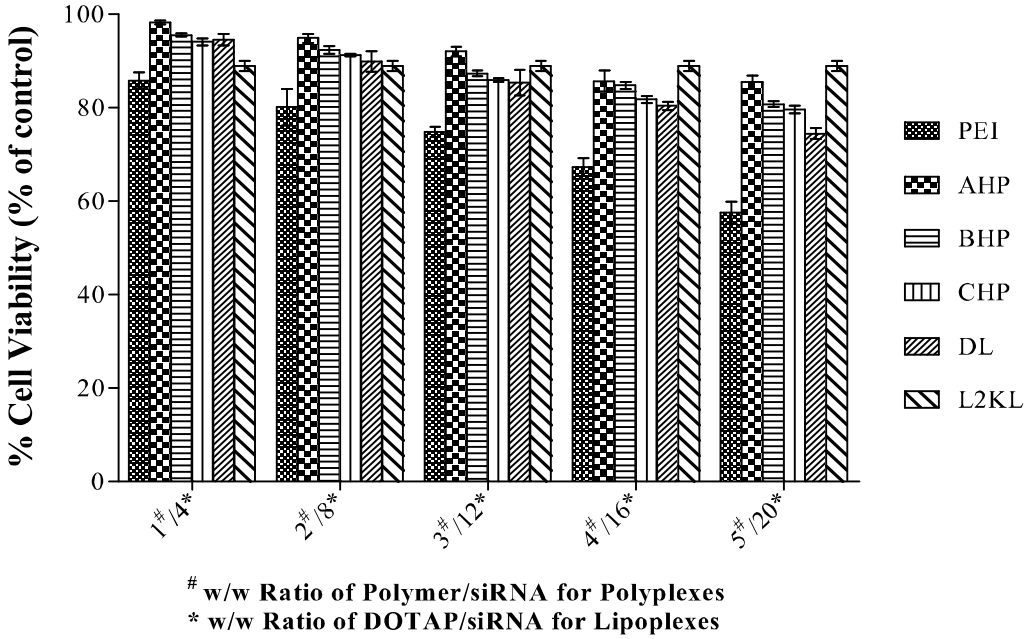

Figure 5.12 Cytotoxicity of AHP, BHP and CHP.

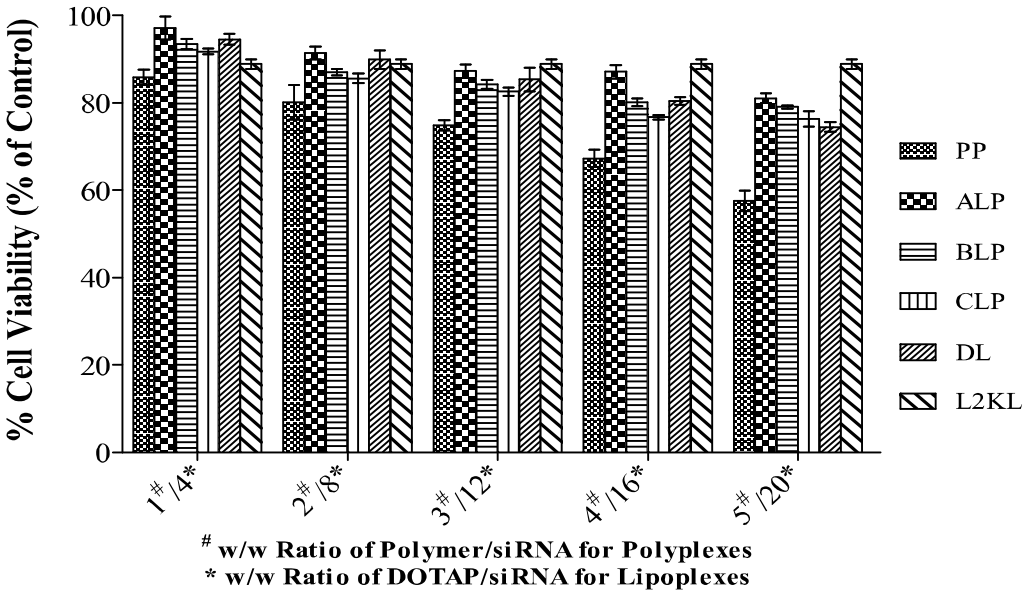

Figure 5.13 Cytotoxicity of ALP, BLP and CLP.

Thorough *in vitro* cell cytotoxicity study for the prepared polyplexes and lipoplexes were carried out. Cytotoxicity of blank (PBS treated control) was used as background. Graphical representation of cell viability against increasing ratio of w/w i.e. ratio of polymer/cationic lipid to siRNA after treatment with developed formulations was assessed by MTT assay as shown in **Figure 5.11, Figure 5.12** and **Figure 5.13**. For comparison of different polyplexes

with lipoplexes, viabilities obtained with DL at different DOTAP/siRNA ratio and viability obtained with L2KL formulation made using a single concentration of L2K as per manufacturer's protocol have been shown in each figure. Also, for legible comparison, DL and polyplexes have been shown based on the cationic species to siRNA w/w ratios, i.e. w/w ratios of DOTAP to siRNA in case of DL lipoplexes and w/w ratios of polymer to siRNA in case of polyplexes. Polyplexes of unmodified PEI reduced the viability to 85.84 ± 1.68% at w/w ratio of 1, while L2K reduced viability to 88.05 ± 0.84% following 48 h of incubation. It was seen that at all w/w ratio, polyplexes developed from synthesized polymers were significantly less toxic on CPA-47 cells than unmodified PEI as well as L2K. Even at higher w/w ratio of 5 and 100 nM siRNA concentration, these polyplexes exhibited significantly less toxicity as compared to L2KL. From the results of MTT assay, it was seen that polyplexes developed from all synthesized polymers were significantly ($p < 0.05$) less toxic than L2KL at w/w ratio of 5.

Polyplexes developed using the PEI having maximum degree of substitution showed highest cell viability and hence least toxicity up to w/w ratio of 5. Further, there was no significant difference in cell viability by changing the type of Boc-amino acid for conjugation to PEI used in the development of polyplex which means that the reduction in overall positive charge by amino acid conjugation and hydrophobicity imparted by use of Boc-amino acids is the major contributor for reduction in cytotoxicity irrespective of type of amino acid used. These results demonstrated a strong dependence of polymer toxicity on the degree of substitution of primary amines with Boc-amino acid residues. Cytotoxicity of cationic polymers is likely due to polymeric aggregation on cell surfaces, impairing important membrane functions. It can be reasoned that a decreased primary amine concentration reduces the charge density of siRNA nanoplexes, thereby lessening cell membrane rupture and consequently reducing cytotoxicity.

Hydrophobic modification of polycations has been shown to be beneficial for gene delivery for a variety of reasons. A few excellent recent examples of studies on hydrophobic modification of a polycation based polymer showed that hydrophobic modification improves the product, but too much hydrophobicity can decrease efficacy (40). Hence, hydrophilic/hydrophobic balance in the delivery vector should be optimum, as it can also affect the transfection. Our results indicate that conjugation of Boc-amino acids mitigates the cytotoxic effects of excess of primary amines in PEI and increases hydrophobic interactions

contributed to increased stabilization of the polyplexes which ultimately leads to alteration in cytotoxicity.

As is the case with cationic polymer based carriers, cationic lipid based carriers for siRNA delivery are also cytotoxic to cells. Cytotoxicity is due to cationic charge mediated cytotoxicity as well as pore formation effects caused by cationic lipids used in preparation of lipoplexes (41). Further, pore formation effect is augmented by fusogenic lipids like DOPE. This causes loss of cellular components as shown with haemolysis study. Prepared DL formulation showed similar cytotoxicity when compared with L2KL up to w/w ratio of 8, while at w/w ratios higher than 8 showed higher cytotoxicity of prepared DL as compared to L2KL. Less cytotoxicity up to w/w ratio of 8 for optimized lipoplexes can be ascribed to better charge neutralization of surface cationic charge of liposomes through incorporation of DPPC and cholesterol as well as stable bilayer formation which will form stable liposomes which would reduce the interaction between DOTAP and DOPE of lipoplexes with cell membrane.

Developed polyplexes from synthesized polymers at all concentrations showed their potential as a novel siRNA carrier with enhanced margin of safety. However, in order to evaluate whether decreased cytotoxicity of prepared polyplexes has led to any changes in cellular uptake in comparison to native PEI, cell uptake studies need to be carried out to verify the transfection of developed nanoplexes. Moreover, transfection of developed formulation was assessed by qualitative and quantitative cell uptake studies.

5.2.4 *In Vitro* Cell Uptake Studies by Confocal Microscopy

Figure 5.14, Figure 5.15, Figure 5.16, Figure 5.17 and **Figure 5.18** show confocal microscopy images depicting cellular uptake of naked siRNA, different polyplex formulations prepared from native PEI and synthesized PEIs, optimized DL formulation and that of commercial transfecting agent, L2KL. Judicious choice of amino acids was done in order to see the effects of conjugation on cellular uptake and transfection through balance between hydrophilicity as well as lipophilicity. Three amino acids with high, moderate and low hydrophobicity were selected. Leucine has high hydrophobicity, alanine has moderate hydrophobicity and histidine has lowest hydrophobicity. However, in order to further augment hydrophobicity while maintaining biocompatibility, concept of Boc protected amino acids was used. Thus, Boc-amino acid conjugation would serve two purposes, firstly, hydrophilic-lipophilic balance would be modified through different amino acids and

secondly, substitution on primary amines of PEI which caused toxicity due to its higher cationic charge (42).

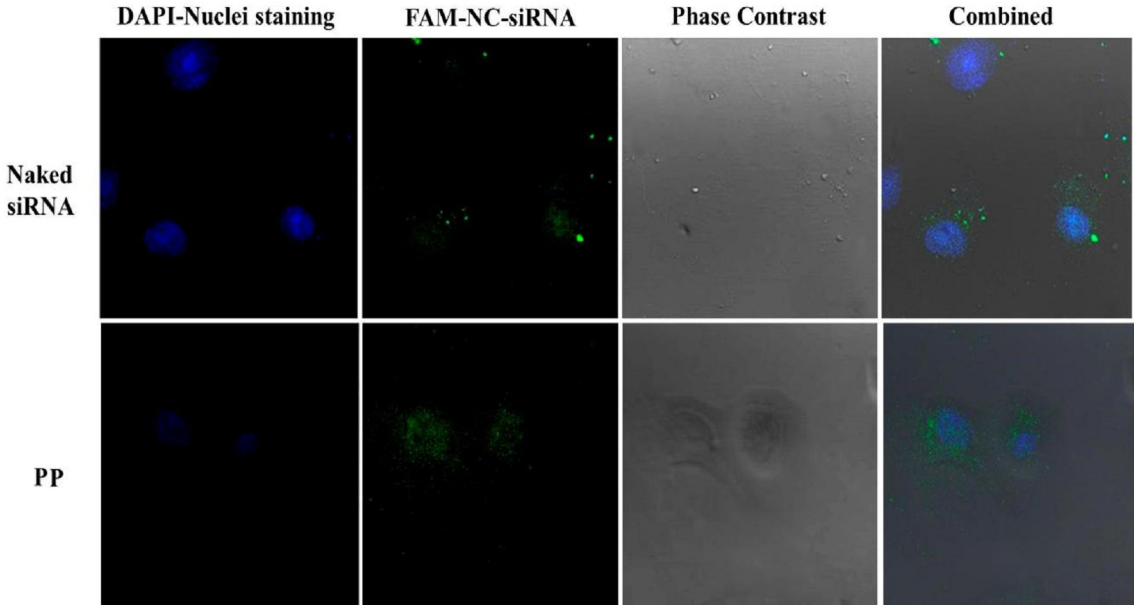

Figure 5.14 Cellular uptake of naked FAM-NC-siRNA and PP by confocal microscopy.

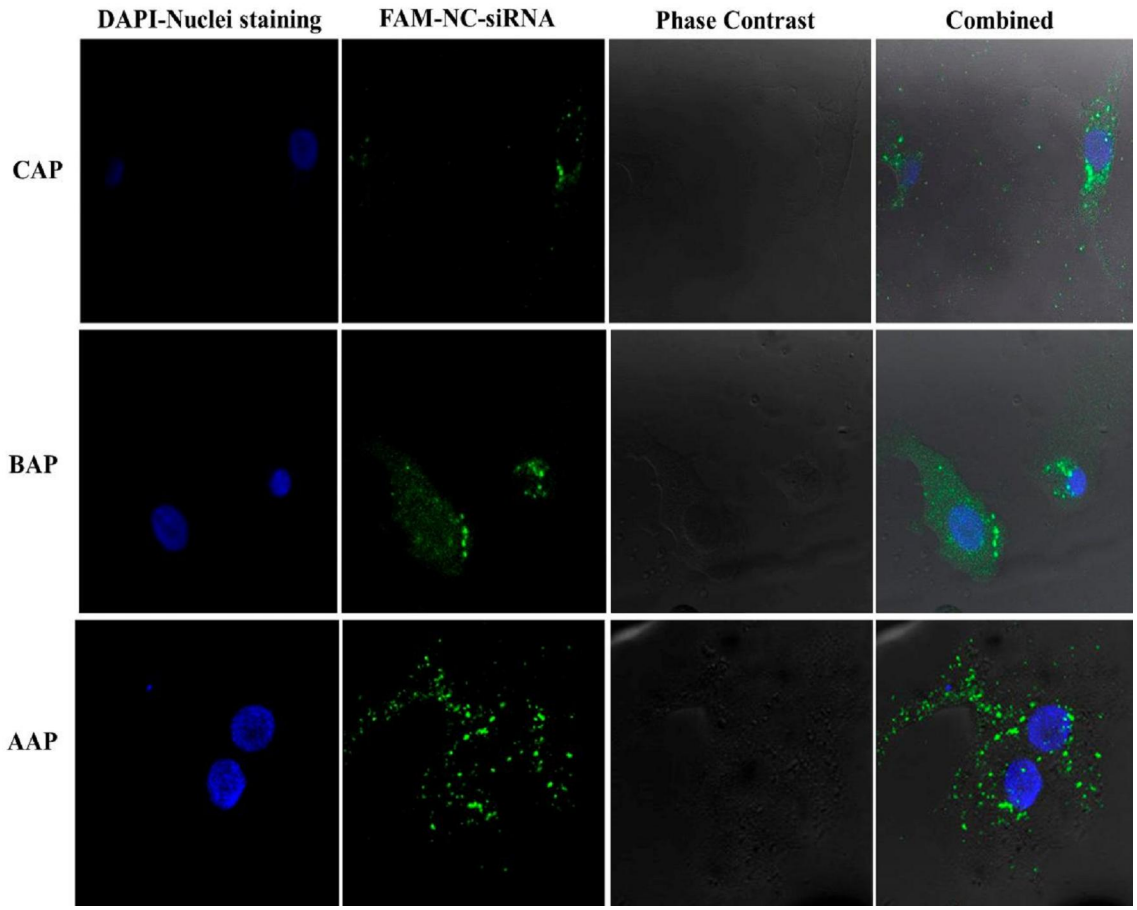

Figure 5.15 Cellular uptake of CAP, BAP and AAP by confocal microscopy.

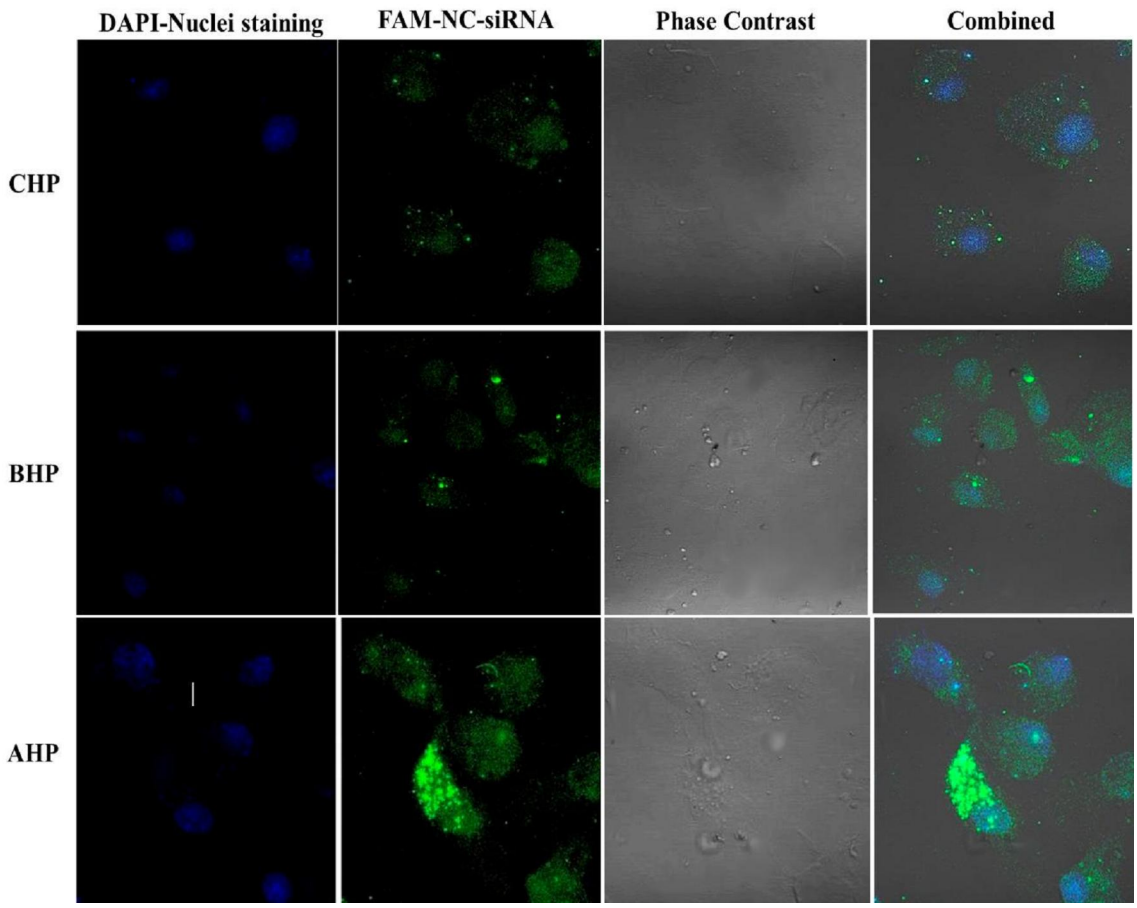

Figure 5.16 Cellular uptake of CHP, BHP and AHP by confocal microscopy.

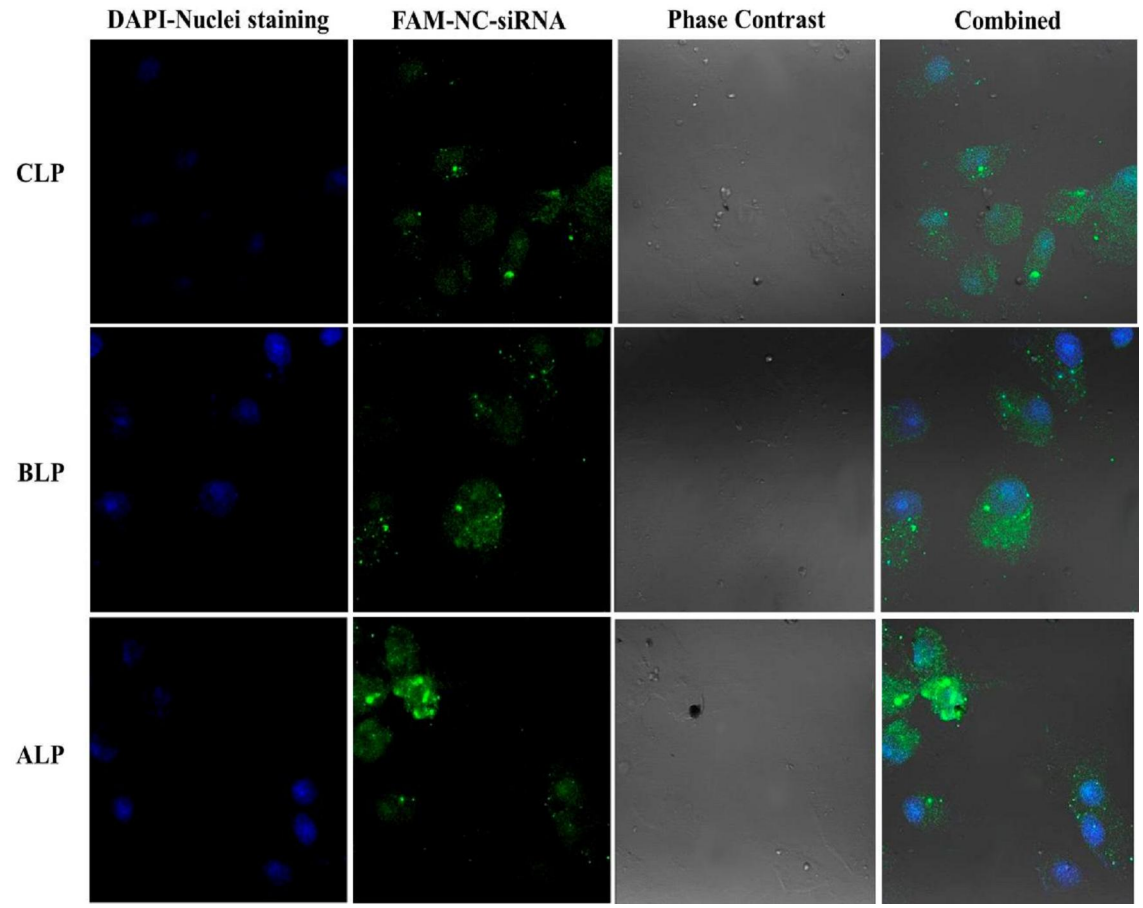

Figure 5.17 Cellular uptake of CLP, BLP and ALP by confocal microscopy.

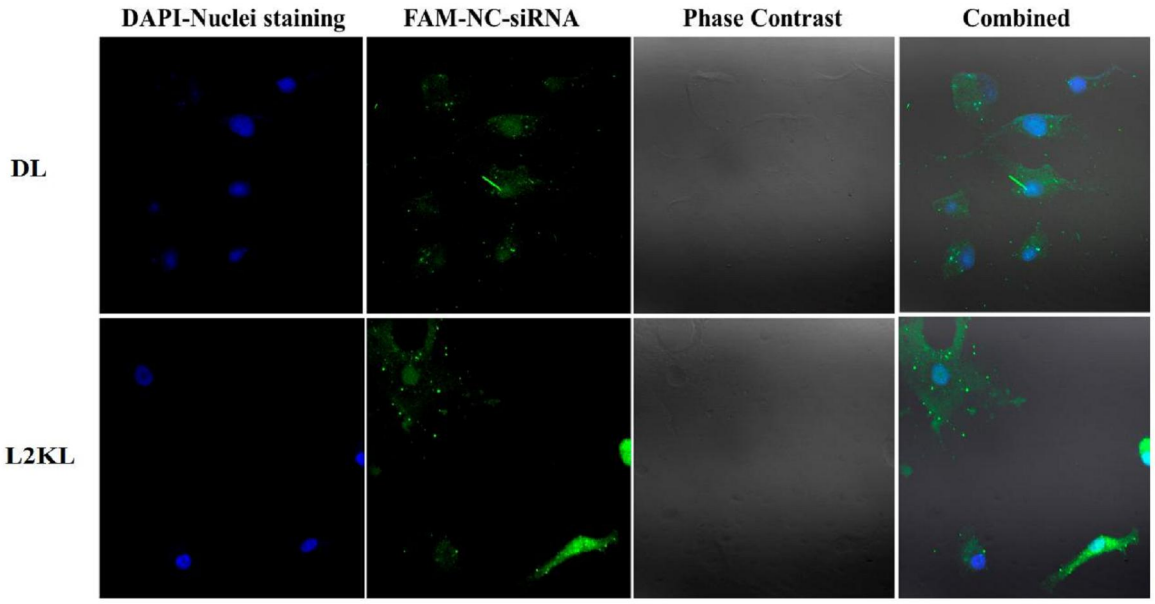

Figure 5.18 Cellular uptake of DL and L2KL by confocal microscopy.

As it can be seen from the **Figure 5.14**, naked siRNA showed negligible cellular uptake, while PEI polyplexes showed marked cellular uptake. Very low uptake of naked siRNA can be imputed to its high molecular weight as well as high hydrophilicity that hinder its passive diffusion through cell membrane. PEI being cationically charged helps condense the negatively charged siRNA while the residual positive charge helps increase its cellular uptake through interaction with negatively charged cell membrane. Such interaction would lead to endocytosis of polyplexes.

Effect of different modified PEIs on cellular uptake is depicted in subsequent images- **Figure 5.15** for Boc-alanine conjugated PEI polyplexes, **Figure 5.16** for Boc-histidine conjugated PEI polyplexes and **Figure 5.17** for Boc-leucine conjugated PEI polyplexes. It can be noted that all modified PEI polyplexes showed higher uptake than that of native PEI polyplexes. This can be attributed to the hydrophobic modification that has been rendered on native PEI through conjugation of Boc-amino acids. It is also apparent from the images that with increasing conjugation level for each Boc-amino acids the cellular uptake went on rising. The images also mark the differences between types of conjugation i.e. at each conjugation level, the cellular uptake was higher for Boc-histidine conjugated PEI polyplexes followed by Boc-leucine conjugated PEI polyplexes and Boc-alanine conjugated PEI polyplexes. This difference can be ascribed to the already discussed effect of imidazole ring of Boc-histidine, partial ionization of which under physiological conditions, would have augmented the uptake of AHP.

In case of lipoplex formulations (**Figure 5.18**), cellular uptake was much higher than that of naked siRNA as well as PEI. DL lipoplexes, as with the polyplexes of PEI, enhanced the cellular uptake through enhanced interaction between cationically charged lipoplexes and negatively charged cell surface and subsequent endocytosis (43). Also, enhanced cellular uptake of lipoplexes would be through DOPE mediated fusion of lipoplexes that will help lipoplexes get through the endosomal membrane (43, 44). Apart from the endosomal escape, some reports also suggest the DOPE mediated fusion of liposomes to the cell membrane leading to direct cytosolic release of lipoplexes (43, 44). All of these mechanisms could be responsible for high cellular uptake of lipoplex formulations.

Considering the endocytosis mechanism, it has been reported that lipoplexes internalize through clathrin-mediated endocytosis, while in case of polyplexes made of PEI, cellular uptake is mediated through clathrin- and caveolae mediated endocytosis (45). Thus,

clathrin- and caveolae-mediated endocytosis that would be taking place at different rates with different conjugated polyplexes and lipoplexes would be responsible for differential uptake results obtained in our study. However, the difference exists in case of transfection i.e. lipoplexes internalized via clathrin-mediated endocytosis show transfection effectiveness, while the same doesn't follow for the transfection effectiveness of polyplexes. Instead, caveolae-mediated endocytosis is effective mechanism of transfection in case of PEI mediated transfection (46).

5.2.5 In Vitro Cell Uptake Studies by Flow Cytometry

Cellular uptake of FAM-NC-siRNA at 100 nM concentration and different nanoplexes at equivalent concentrations were subjected to flow cytometric analysis for quantification of cellular uptake. **Figure 5.19, Figure 5.20, Figure 5.21**, **Figure 5.22** and **Figure 5.23** show 2D histograms as well as Dot plots of FACS analysis of cellular uptake of naked siRNA, and nanoplexes results of which are shown in **Table 5.10.**

.

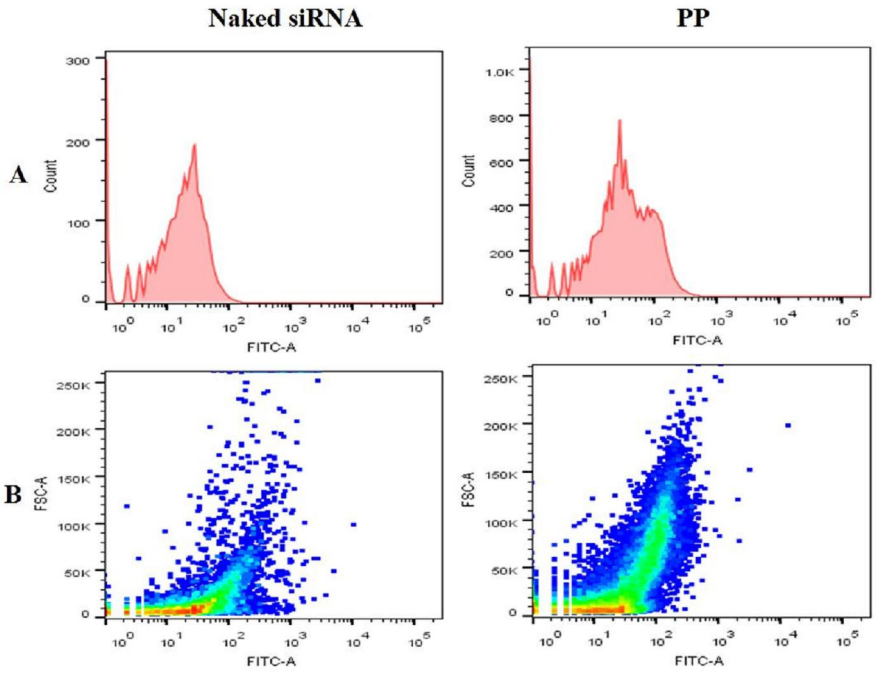

Figure 5.19 2D histograms (A) and dot plots (B) of cell uptake of naked siRNA and PP in CPA-47 cells by FACS.

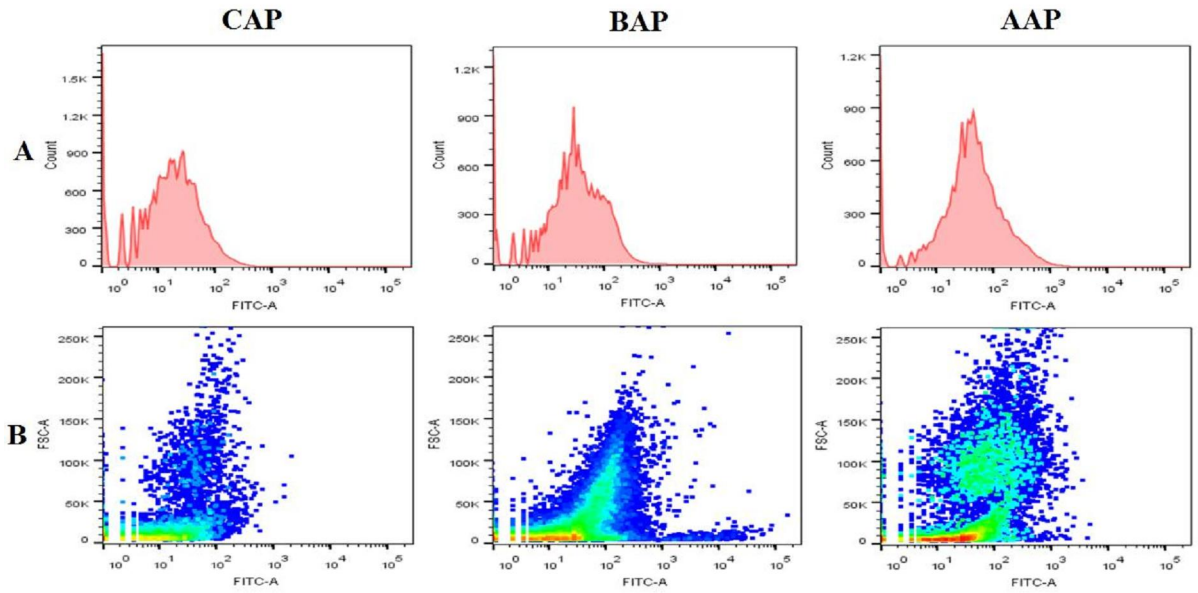

Figure 5.20 2D histograms (A) and dot plots (B) of cell uptake of CAP, BAP and AAP in CPA-47 cells by FACS.

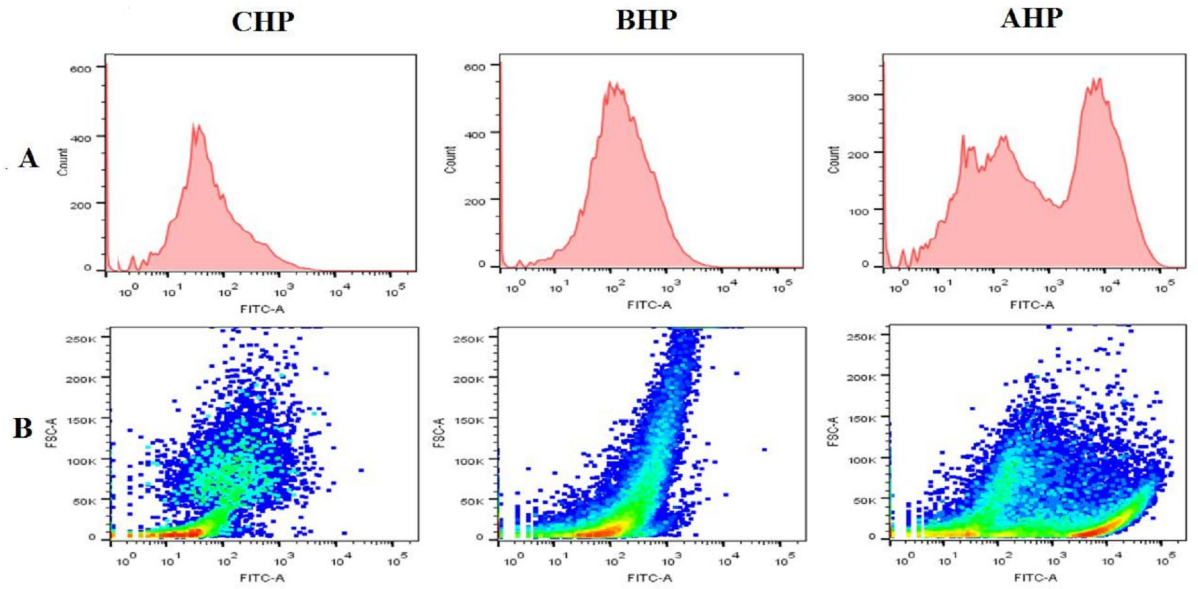

Figure 5.21 2D histograms (A) and Dot plots (B) of cell uptake of CHP, BHP and AHP in CPA-47 cells by FACS.

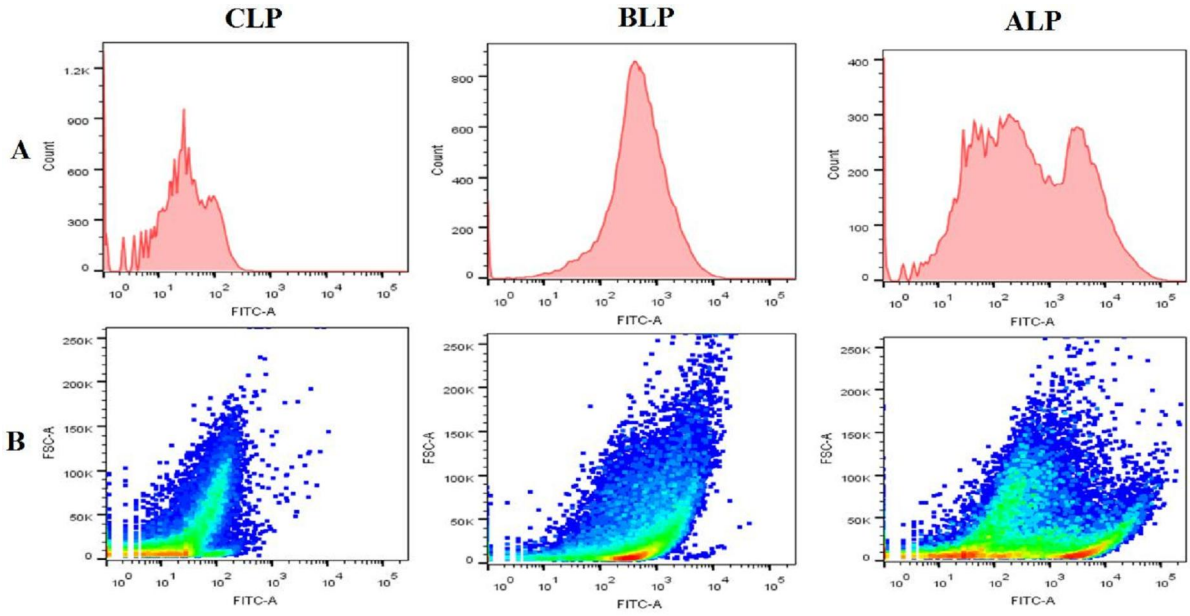

Figure 5.22 2D histograms (A) and dot plots (B) of cell uptake of CLP, BLP and ALP in CPA-47 cells by FACS.

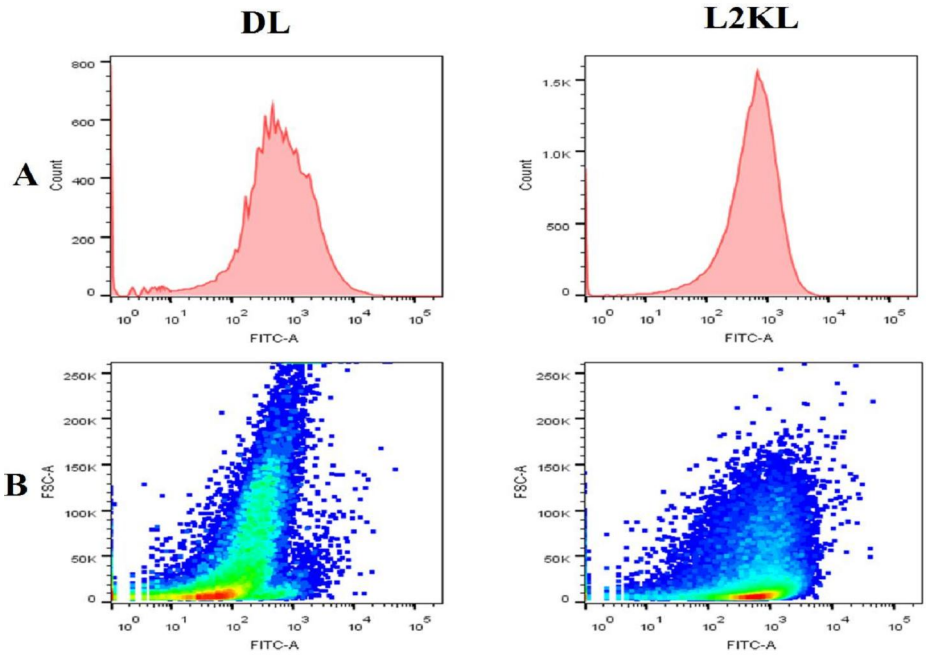

Figure 5.23 2D histograms (A) and dot plots (B) of cell uptake of DL and L2KL in CPA-47 cells by FACS.

Table 5.10 Uptake of various formulations in CPA-47 cells

Formulations	Mean Fluorescent Intensity
Naked siRNA	10.90±1.78
PP	64.16±1.39
AAP	73.25±0.38
BAP	72.20±0.82
CAP	68.28±0.34
AHP	84.36±0.99
BHP	77.63±0.59
CHP	72.76±1.29
ALP	75.14±0.41
BLP	74.96±1.15
CLP	70.28±1.25
DL	67.81±0.61
L2KL	66.11±0.40

*Values are represented as mean±SD, n=3.

Figure 5.24 shows MFI inside cells treated with naked FAM-NC-siRNA and different nanoplexes thereof. Naked siRNA showed very low level of uptake while PEI formulations led to higher uptake inside cells due to cationic charge mediated endocytosis.

Among the PEI formulations, all modified polymers exhibited higher cellular uptake as compared to native PEI. With each Boc-amino acid type, as the conjugation level increased the cellular uptake was found to increase. i. e. regardless of the amino acid type, cellular uptake of PEI and modified PEIs exhibited following pattern:

$$AXP \geq BXP > CXP > PP$$

(where X represents the amino acid type i.e. A-alanine, H-histidine and L-leucine)

Among the amino acid types, at each conjugation level, the cellular uptake exhibited following pattern:

Boc-histidine-PEI>Boc-leucine-PEI>Boc-alanine-PEI.

Differences existing among different modified polymers can be attributed to the balance of hydrophobicity and cationic charge, both of which are prime governors of the cellular uptake (42). Hydrophobic modification of PEI with Boc-amino acids increases the cellular uptake of polyplexes since all synthesized polymers showed increased cellular uptake as compared to PEI. PEI modified with Boc-alanine showed low uptake when compared with PEI modified with Boc-leucine. This can be due to the higher hydrophobicity of Leucine as compared to alanine. Thus, higher uptake of Boc-leucine-PEI can be ascribed to both leucine's inherent hydrophobicity which is further augmented by Boc protection. Our results are in agreement with previous report on polypropyleneimine which showed higher uptake after modification with Boc protected glycine (47). However, looking at the conjugation level, initial increase in conjugation level increased cellular uptake which was not enhanced on further increase in conjugation as seen for Boc-alanine and Boc-leucine modified PEIs which showed no significant increase in cellular uptake as the conjugation increased from BAP to AAP and BLP to ALP. This might be due to extensive hydrophobic modification which leads to impaired uptake (42). In contrast, in case of Boc-histidine-PEI polyplexes, increase in conjugation level (from CHP to AHP) caused significant rise in cellular uptake instead of levelling off. It might be perceived that increased hydrophobicity was further accompanied by increased imidazole content also, partial ionization of which would maintain the hydrophilicity of the polymer. And hence, among all PEI formulations, Boc-histidine conjugated PEI led to highest cellular uptake in pulmonary artery endothelial cells. This can be justified by a perfect balance between cationic charge (generated through partial ionization of imidazole ring of histidine) and hydrophobicity rendered through Boc modification governing the cellular uptake of formulation, former allowing interaction with negatively charged cell surface and hydrophobicity accounting for augmentation of uptake through caveolae-mediated uptake as mentioned before.

Both the lipoplex formulations also showed more than 65% cellular uptake with that of DL higher than L2KL. However, the difference in uptake was not statistically significant. Higher cellular uptake of both lipoplex formulations can be ascribed to high surface charge density mediated endocytosis and DOPE mediated membrane fusion as described earlier.

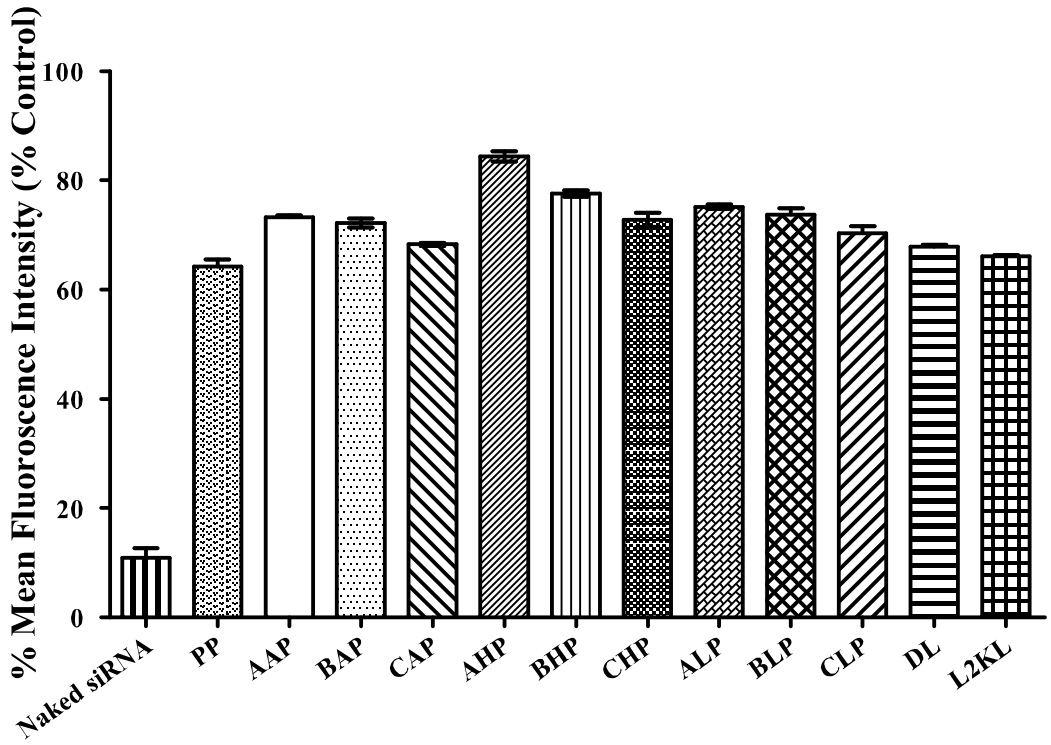

Figure 5.24 %Mean fluoroscence intensity in CPA-47 cells by FACS.

5.1.5.6 *In Vitro* Gene Expression Study by Real Time PCR

From the results of cytotoxicity studies and cellular uptake studies, three polyplex formulations i.e. AAP, AHP and ALP and both lipoplex formulations i.e. DL and L2KL were further evaluated for gene silencing efficacy. In case of polyplexes, AHP was the obvious choice for gene transfection due to higher cellular uptake as compared to other formulations. However, in case of polyplexes made from Boc-alanine and Boc-leucine modified PEIs, though cellular uptake was not increased when conjugation level was increased from BAP to AAP and from BLP to ALP, AAP and ALP were chosen for transfection studies due to their low cytotoxicity.

Table 5.11 Gene expression study of different formulations in CPA-47 cells

siRNA/Formulations	Gene expression (% control)		
	25 nM	**50 nM**	**75 nM**
NC-siRNA	99.37±1.24	99.84±0.11	99.43±0.69
Naked FGF-2 siRNA	101.38±1.36	98.01±1.33	97.10±3.75
PP	89.62±2.47	66.02±1.65	41.91±1.49
AAP	78.47±2.66	56.12±2.47	33.74±2.13
AHP	68.78±2.71	40.70±2.43	22.14±2.28
ALP	76.41±3.48	49.52±2.60	28.46±1.69
DL	85.58±2.31	62.12±2.07	38.89±1.61
L2KL	83.85±2.69	60.68±1.42	35.62±1.31

*Values are represented as mean±SD, n=3.

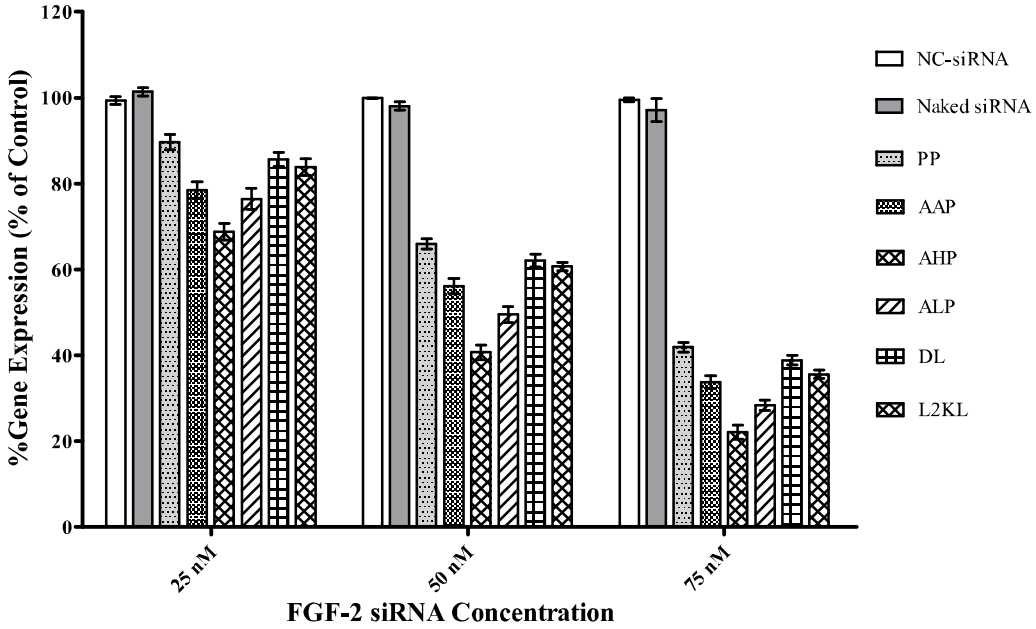

Figure 5.25 Gene expression study of different formulations in CPA-47 cells.

Table 5.11 and **Figure 5.25** represent the siRNA transfection efficiency of different nanoplexes as compared to that of naked siRNA. mRNA expression levels were estimated as a % of FGF-2 mRNA expression of PBS treated control. Naked siRNA reduced this expression, however, at very low extent (<10%). And as it is apparent from the figure, all nanoplexes showed very high mRNA silencing efficiency i.e. reduced target gene expression.

In addition to gene silencing due to siRNA and its formulations, in order to check whether the gene silencing was due to only FGF-2 siRNA and not due to any off-target effects of siRNA, we also evaluated the gene silencing due to scrambled sequence siRNA. However, scrambled sequence siRNA did not cause any suppression of FGF-2 mRNA, confirming the sequence specificity of siRNA for target mRNA degradation.

Comparing different formulations, at each siRNA concentration evaluated, the gene expression was in concordance with the cellular uptake studies. High gene silencing by PEI and modified PEIs can be attributed to the high cellular uptake and proton sponge effect contributed by the modified polymers. Among the screened polyplexes, AHP showed maximum gene silencing, followed by ALP, AAP and native PEI polyplexes. High silencing efficiency of AHP can be attributed to combined effects of hydrophobic modification due to Boc-histidine and contribution from imidazole in proton sponge effect which protects siRNA through buffering effect and helps siRNA escape from the endosomal environment. ionizable imidazole moieties (<7.4 pH) of Boc-histidine act as replacement for the primary amino functions lost during the modification. However, this was not the case with AAP and ALP, where only hydrophobic modification and contribution by amines groups of PEI backbone would be responsible for transfection.

In case of lipoplex formulations, optimized DL formulations showed similar transfection efficiency as that of L2KL. However, the efficiency of both lipoplexes was lower than that of polyplexes. This can be ascribed to the absence of proton sponge effect which both lipoplexes were lacking. However, the high transfection efficiency approaching that of PEI can be attributed to the cationic charge mediated uptake, DOPE mediated endosomal membrane fusion as well as direct fusion to cell membrane leading to cytosolic release of siRNA. Once internalized into endosomes, interaction between the cationic lipoplexes and negatively charged endosomal membrane takes place in which anionic phospholipids of the endosomal membrane diffuses into the lipoplex bilayer forming neutral ion pairs with positively charged phospholipids of lipoplex. This process helps the fusion between the endosomal and lipoplex membrane as well as displacement of siRNA molecules form the surface of lipoplexes and hence causes cytosolic release of siRNA (48-50). The process of membrane fusion and dissociation of siRNA from lipoplexes is further aided by the DOPE which forms a hexagonal phase especially at acidic pH due to its ethanolamine head group (51).

5.2.7 *In Vitro* Cell Line Studies in HCPA-47 Cells

5.2.7.1 *In Vitro* Cytotoxicity Study

From the results of cytotoxicity, cellular uptake and gene transfection studies, PP, AAP, AHP ALP, optimized DL and L2KL were further evaluated for their cytotoxicity in hypoxia induced cell line. **Figure 5.26** shows effect of various nanoplexes on viability of HCPA-47 cells. As it can be seen, cytotoxicity followed similar pattern that was observed in normoxic cell line. PEI showed highest cytotoxicity as compared to all other polyplexes as well as lipoplexes.

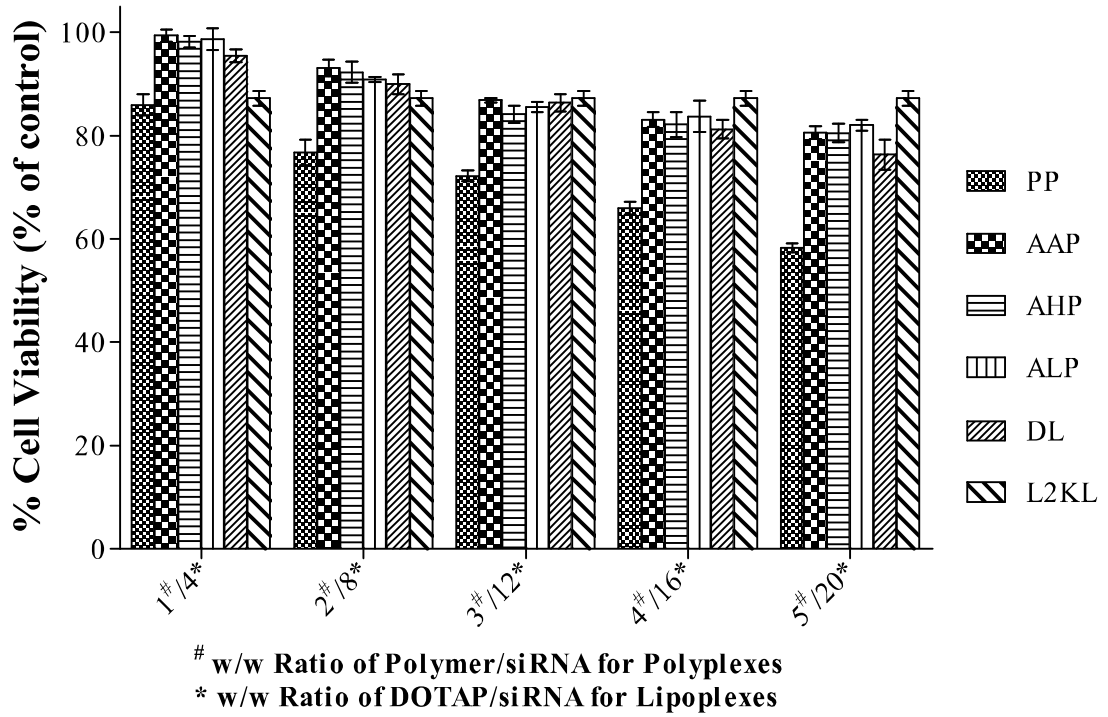

Figure 5.26 Cytotoxicity of nanoplexes in HCPA-47 cells.

As described earlier, cytotoxicity of PEI polyplexes can be attributed to charge based aggregation and membrane fusion of cells as well as pore formation and that of lipoplexes can be ascribed to the pore formation due to cationic lipids and DOPE as well as charge mediated cytotoxicity.

5.2.7.2 *In Vitro* Cellular Uptake Studies

To confirm that the cellular uptake in hypoxic cells was at par with that in normoxic cells, cellular uptake studies on cells grown in hypoxic conditions were also performed.

However, as expected, cellular changes that might have taken place in hypoxic pulmonary arterial endothelial cells did not cause any changes in the uptake of PEI and modified PEI polyplexes as well as DL lipoplexes. As shown in **Figure 5.27**, confocal microscopy confirmed that modification of PEI with Boc-histidine led to highest cellular uptake of polyplexes followed by that of PEI modified with Boc-leucine and Boc-alanine. Both lipoplex formulations also showed higher uptake than PEI polyplexes. However, it was lower than that observed with modified PEI polyplexes.

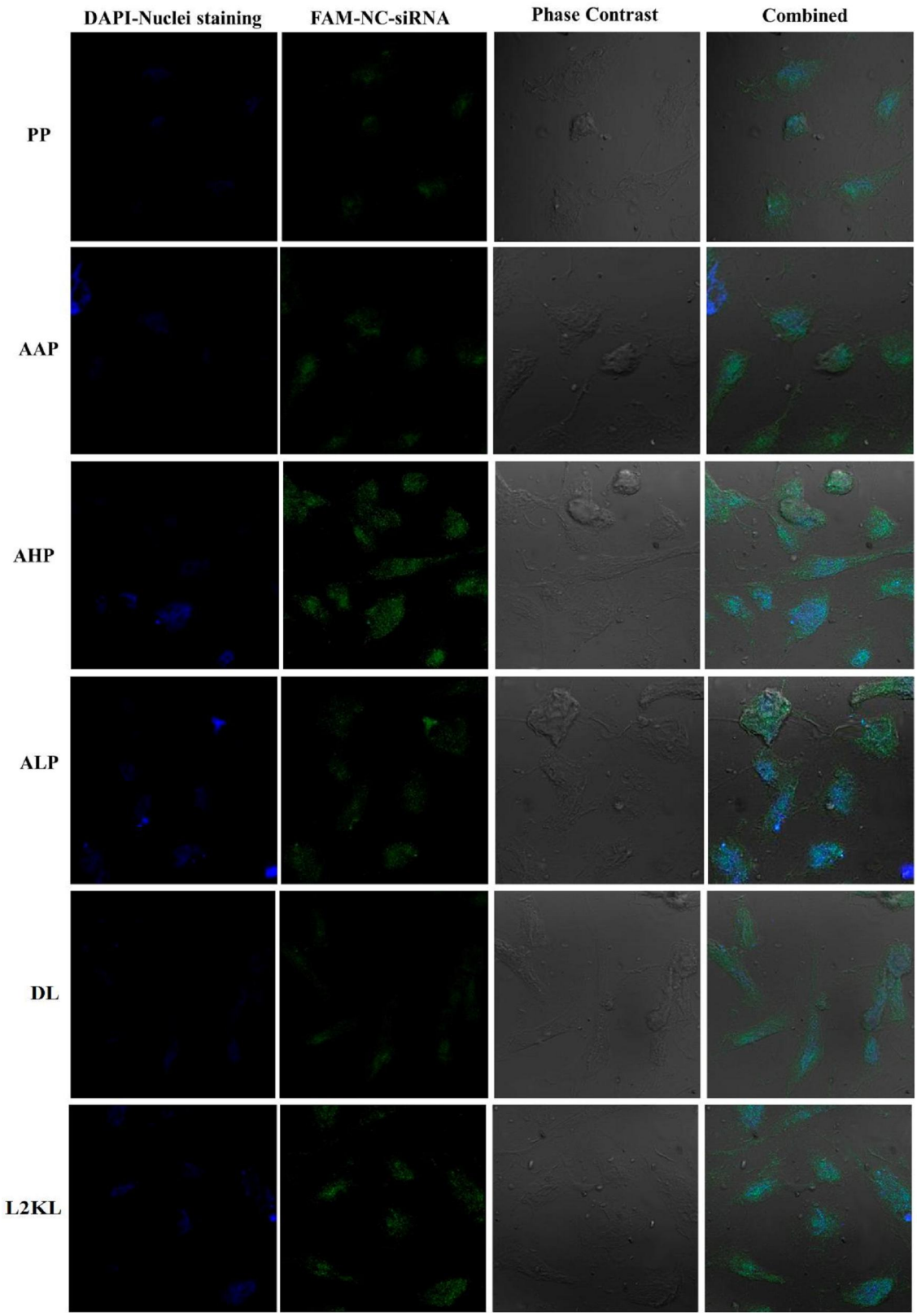

Figure 5.27 Cell uptake of screened formulations in HCPA-47 cells by confocal microscopy.

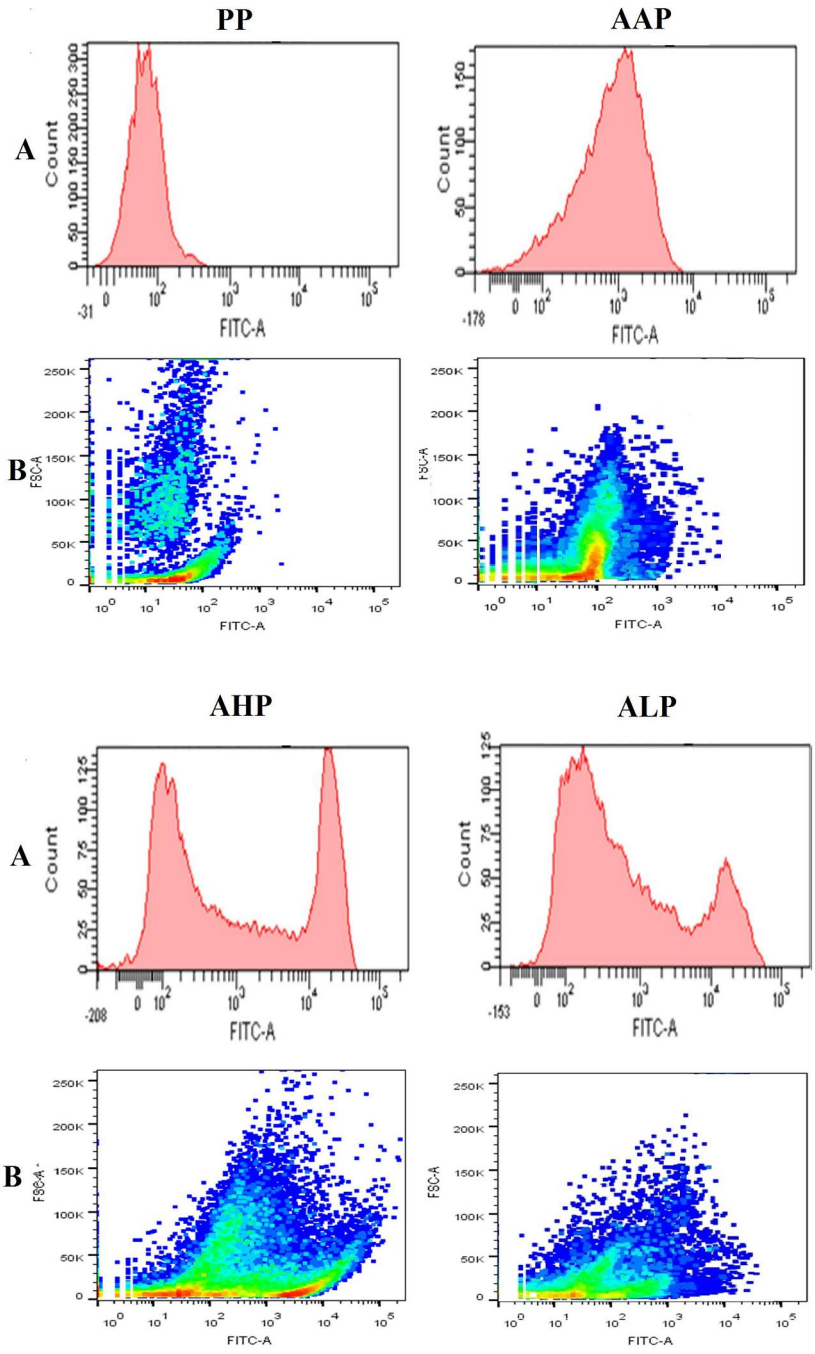

Figure 5.28 2D histograms (A) and dot plots (B) of cell uptake of PP, AAP, AHP and ALP in HCPA-47 cells by FACS.

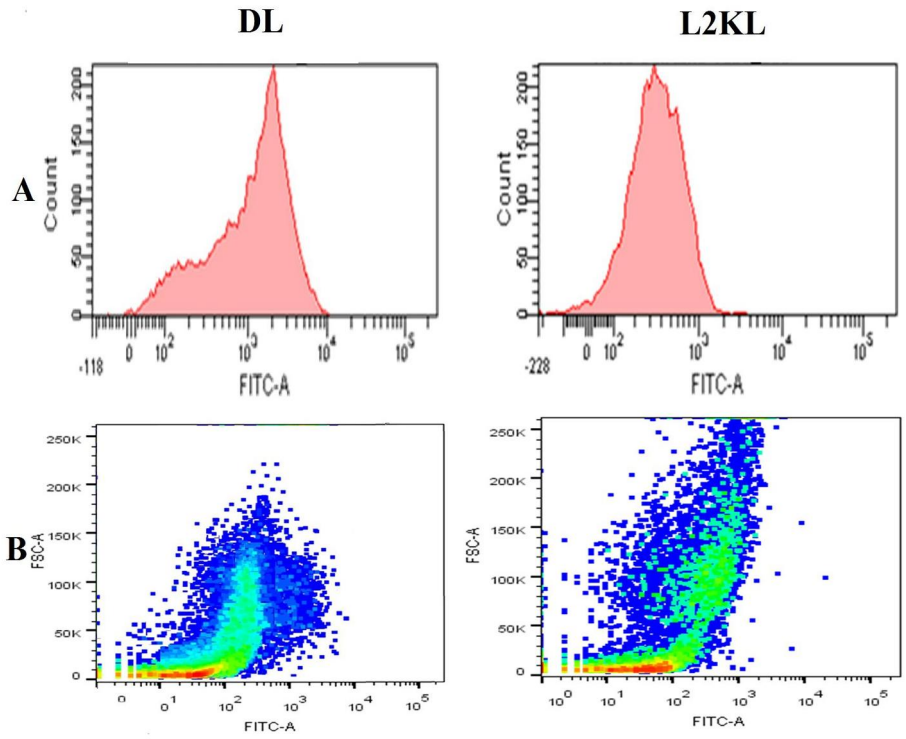

Figure 5.29 2D histograms (A) and dot plots (B) of cell uptake for DL and L2KL in HCPA-47 cells by FACS.

Table 5.12 Cell uptake of screened formulations in HCPA-47 cells by FACS.

Formulation	% Cellular Uptake (%MFI as compared to control)
PP	68.567±1.491
AAP	75.263±0.866
AHP	87.963±1.115
ALP	79.487±0.781
DL	67.387±1.445
L2KL	67.187±2.786

*Values are represented as mean±SD, n=3.

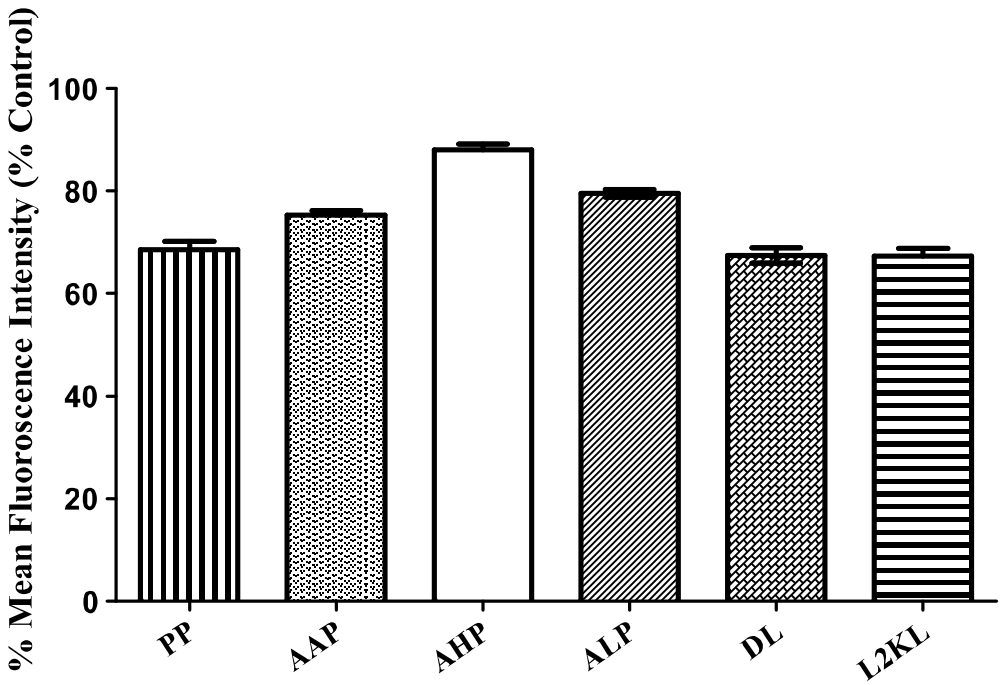

Figure 5.30 Cell uptake of screened formulations in HCPA-47 cells by confocal microscopy.

Quantitative estimation of cellular uptake obtained using flow cytometry (**Figure 5.28, Figure 5.29** and **Figure 5.30**) also corroborated the results obtained using confocal microscopy. **Table 5.12** shows cellular uptake of different formulations in hypoxic cells relative to PBS treated cells. The trend of cellular uptake observed in normotoxic cells i.e. AHP>ALP>AAP>DL≥L2KL>PP was still observed in hypoxic cells as well and can be justified by the same fundaments of hydrophobicity and charge in case of polyplexes and charge and lipid composition in case of lipoplexes. However, unlike lipoplexes, all polyplexes showed higher uptake in hypoxic conditions than that under normoxic conditions. This might be due to acidification of the cell culture by acidic metabolic products of cells produced under hypoxic conditions (52). Such acidification would cause ionization of the secondary amino functions of the polymers during incubation of polyplexes with cells and hence result in charge mediated uptake of these polyplexes. However, this was not the case with the cationic lipoplexes made of phospholipids (DOTAP and DOTMA) which are ionized at all pH. So there were no changes in the cellular uptake of DL.

5.2.7.3 *In Vitro* Gene Expression Study by RT-PCR

Hypoxic conditions lead to expression of stress cytokines like FGF-2. Hence, the FGF-2 mRNA knockdown by siRNA was evaluated in hypoxic conditions. As in the case of gene expression studies under normoxic conditions, 25 nM, 50 nM and 75 nM siRNA concentrations were also used for gene expression studies under hypoxic conditions.

Table 5.13 Gene expression in HCPA-47 cells after treatment with various formulations

siRNA/Formulations	Gene expression (% of PBS control)		
	25 nM	50 nM	75 nM
NC-siRNA	99.87±0.56	99.33±0.50	99.68±0.30
Naked FGF-2 siRNA	98.48±1.72	94.74±2.76	94.10±3.42
PP	77.25±2.28	45.23±0.98	28.12±2.58
AAP	64.69±67.43	31.36±34.59	19.65±22.53
AHP	51.35±49.10	22.95±25.36	8.68±13.98
ALP	61.32±63.51	31.45±27.87	16.25±20.68
DL	76.35±73.59	41.45±39.15	27.65±29.94
L2KL	75.69±76.94	37.69±40.37	23.65±26.69

*Values are represented as mean±SD, n=3.

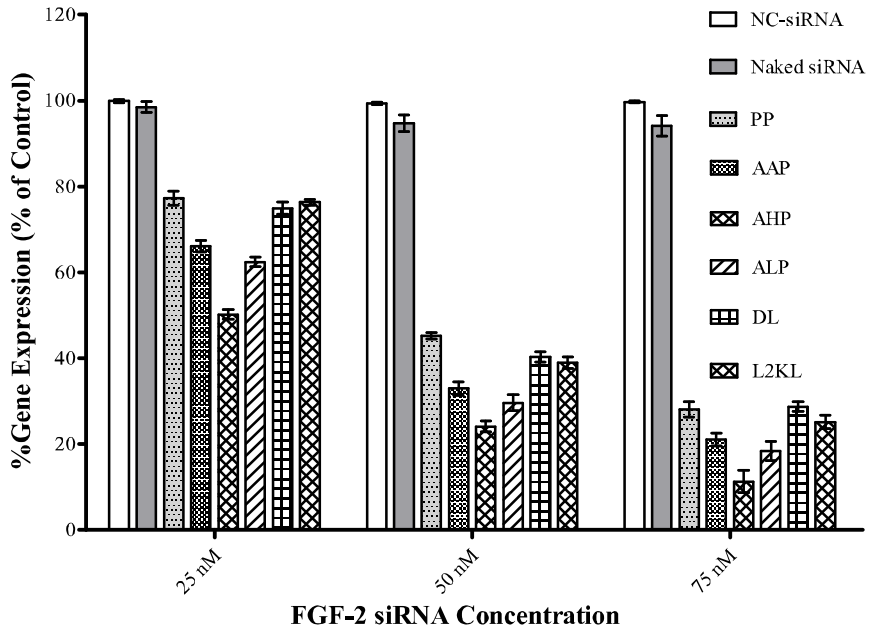

Figure 5.31 % Gene expression in HCPA-47 cells after treatment with various formulations.

Trend observed in gene transfection efficiency in HCPA-47 cells was in concordance with that observed in normoxic cells i.e. decreasing in the order of AHP>ALP>AAP>PP>DL~L2KL (**Figure 5.31** and **Table 5.13**). However, the transfection efficiency in terms of percentage mRNA knock down was increased for each polyplex as compared to normoxic conditions. This can be justified by the fact that cells grown in hypoxic conditions for longer periods show lower (acidic) extracellular as well as cytosolic pH due to metabolic defects induced due to stress response (53). This might cause ionization of amine groups of pH sensitive PEI causing tightening of PEI-siRNA complex. However, the tendency of such ionization would be lesser with modified PEIs than with native PEI, due to steric hindrance which obstructs protonation of secondary amino functions buried inside the polymer structure as well as less number of primary amino functions in the former. However, such ionization in case of polyplexes of native PEI would cause more tightening of the complex as compared to modified PEI, due ionization of secondary amino groups. Additionally, FGF2 expression levels are high under hypoxic conditions (54), depicting high levels of FGF-2 mRNA levels inside the cells. Hence, as mRNAs molecules are available for siRNA molecules the siRNA concentrations used may not be sufficient enough to cause gene silencing to an extent as expected from the gene silencing study carried out in normoxic cells. In other words, our results support, in a way, the findings of previous studies that show higher FGF-2 expression in hypoxic conditions.

In contrast to polyplexes, reduction in gene transfection efficiency of lipoplexes can only be ascribed to the high FGF-2 mRNA levels induced by hypoxia. This difference between the polyplexes and lipoplexes, can be justified by the fact that pH of the cytosolic compartment would not be affecting the siRNA release from the lipoplexes due to inherently quaternary amino functions of cationic phospholipids that would not be responsible in pH depended ionization affecting binding and release. However, in this case, the release would only be dependent on the release of siRNA from the surface adsorbed siRNA through displacement by negatively charged endosomal membrane components during fusion (48-50). Further, low transfection efficiency of lipoplex formulations as compared to polyplex formulations indicate that PEI based formulations are more efficient vectors as compared to cationic lipid based vectors suggesting significant role of proton sponge effect in endosomal escape as compared to membrane fusion and membrane rupture by lipoplexes.

5.2.8 Heparin Polyanion Competition Assay

As described earlier, electrostatic interaction between the siRNA and cationic polymer/phospholipid renders stability to nanoplexes, respectively. It has been reported that heparin causes concentration-dependent dissociation of DNA from polyplexes as well as lipoplexes (24). Similar could be the case with siRNA polyplexes as well as lipoplexes. However, the stability of nanoplexes is dependent on the number of charge per complexed molecule i.e. DNA vs. siRNA (39). Additionally, it has been shown that the polymeric siRNA (above ~ 300 bps) maintained stable complexes with PEI even in the presence of heparin (55). This makes it apparent that siRNA based formulations would be much influenced by presence of polyanions like heparin. Hence, heparin competition assay was performed to estimate the stability of prepared formulations on exposure to *in vivo* conditions where formulation is to face polyanions. Additionally, this would also give the idea about whether the formulations were made at appropriate N/P or w/w ratio as it directly extrapolates to their transfection efficiency (24).

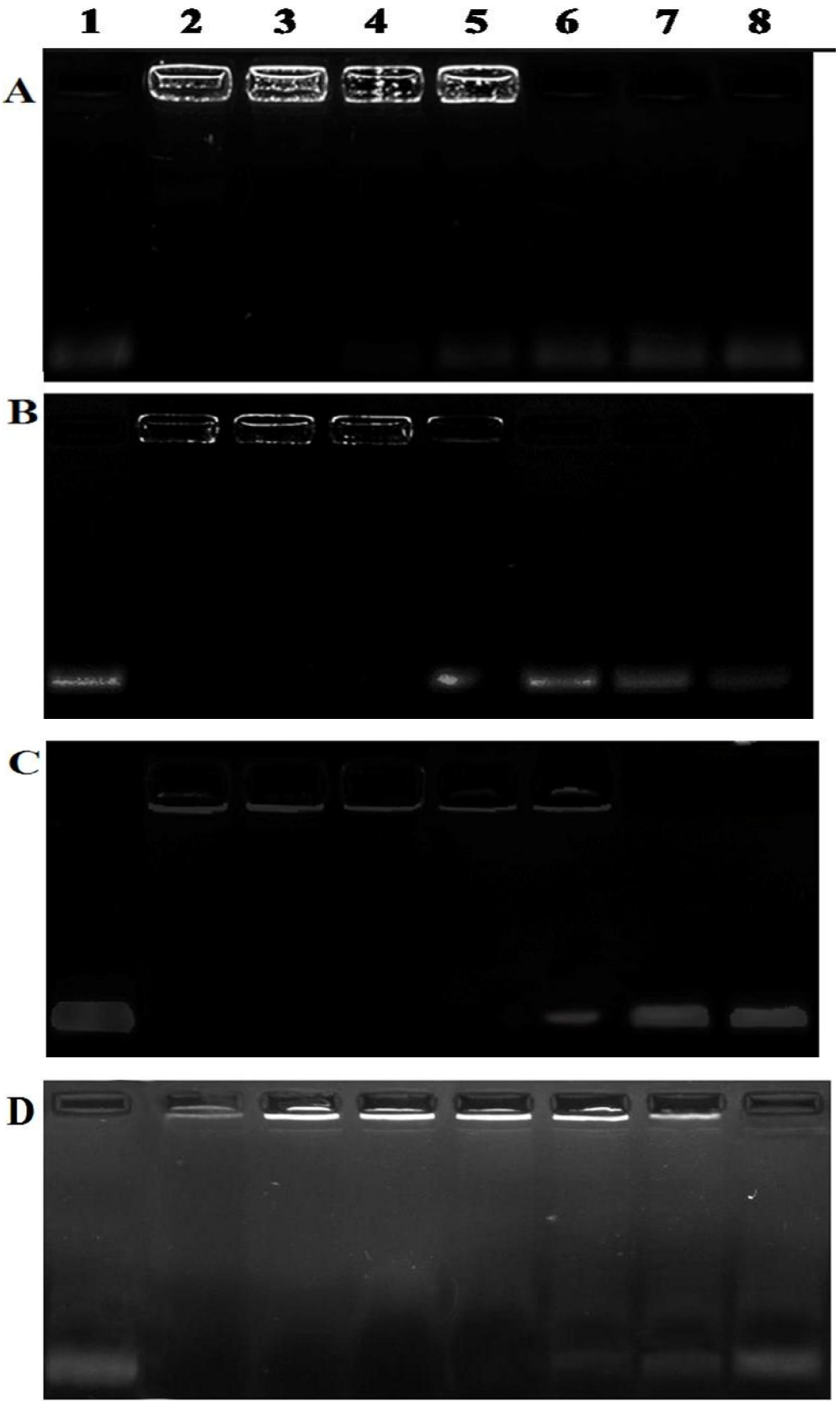

Figure 5.32 Heparin polyanion competition assay A) AAP; B) ALP; C)AHP and D) DL.

After incubation with different concentration of heparin, the amount of heparin required for releasing the total amount of siRNA from nanoplexes was determined by gel electrophoresis (**Figure 5.32**). As it can be seen, siRNA was observed in the sample wells when it was not released from the formulations at that specific concentration of heparin (56, 57). Rise in concentration of heparin led to increase in siRNA band density indicating concentration dependent release of siRNA from formulations. This might be attributed to the displacement of siRNA molecules by heparin molecules.

Figure 5.32 shows that complete siRNA was released from ALP and AAP when heparin concentration was 0.5 mg/mL or higher and from AHP at heparin concentration of 0.6 mg/mL. The amount of heparin needed to release siRNA from the AHP was quite higher than that for ALP and AAP. GAG concentration in human serum at its higher end is 20 μg/mL. Heparin concentration required to release siRNA from polyplexes was way far higher than present in human blood indicating their apparent stability *in vivo*. Additionally, various GAGS present in lungs include hyaluronan, heparin sulphate, dermatan sufate and chondroitin sulphate (58). However, stability of formulations at high heparin levels justifies their stability in bronchoalveolar fluid as well.As evident for AHP, the synthesized polymer AH could hinder siRNA release by heparin, possibly by entrapping siRNA inside strong complexes with imidazole ring that provided some additional protection. Additionally, hydrophobic modification could also be accounted for the stability of polyplexes. DL also showed good protection against heparin (**Figure 5.32**) competition and showed that it can be a good delivery vehicle in gene delivery. Higher stability of DL can be accounted for the PEGylation rendered on the surface of the DL through the use of DSPE-mPEG-2000 that would sterically hinder the direct interaction between the DL and polyanion. Thus, developed nanoplexes showed good resistant to disruption by heparin depicting their stability *in vivo*.

5.2.9 Serum Stability Study

Non-viral gene delivery vectors like nanoplexes should have the property to protect siRNA from degradation by RNAses, especially those present in serum if administration is meant for intravenous administration or in organs where negatively charged proteins can affect the stability of formulation. In order to evaluate potential of prepared nanoplexes to protect siRNA from aforesaid degradation mechanisms, serum stability studies were carried out by incubating formulations under high serum conditions (50% v/v). Gel electrophoresis image

showing siRNA analysis of different formulations at different time points is shown in **Table 5.14** and **Figure 5.33.**

Table 5.14 Serum stability of nanoplexes as compared to naked siRNA

Time (hr)	% siRNA retained				
	Naked siRNA	AAP	AHP	ALP	DL
0	100.00	100.00	100.00	100.00	100.00
1	71.56±3.45	96.85±2.36	98.65±2.65	98.79±2.25	99.03±1.45
2	42.39±2.89	95.29±1.95	97.16±2.75	97.56±3.69	98.26±2.15
4	12.96±4.65	94.55±3.65	96.56±2.10	96.04±5.12	96.56±1.75
8	Not detectable	89.79±4.02	92.36±1.09	92.13±2.22	92.96±4.12
16		82.27±1.95	86.01±3.94	85.29±1.95	87.26±2.65
20		77.36±4.65	83.25±1.58	79.23±3.53	83.02±2.09
24		73.82±2.54	79.65±1.95	74.55±1.29	77.33±1.49

*Values are represented as mean±SD, n=3.

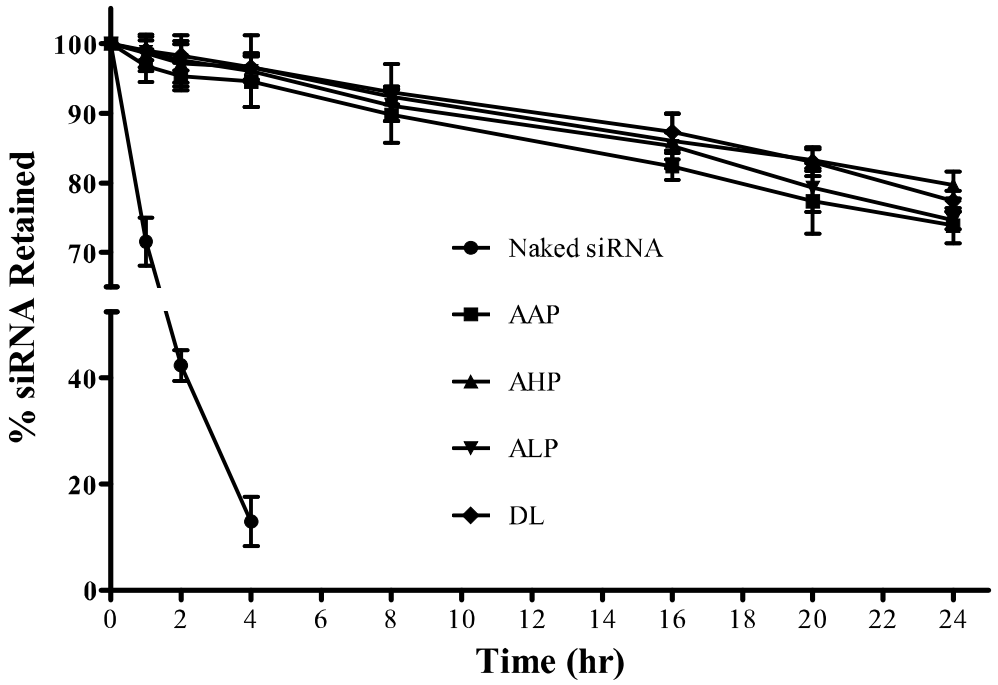

Figure 5.33 Serum stability of nanoplexes as compared to naked siRNA.

Gel electrophoresis performed to evaluate the stability of developed formulations showed that developed nanoplexes were able to protect FGF-2 siRNA from serum nuclease mediated degradation. As shown in **Figure 5.33**, naked siRNA started to degrade in serum significantly from the start with approximately 30% degradation within an hour which reached almost complete degradation within 8 hr of incubation. The degradation observed was in concordance with published data by Judge et al. (59). However, in case of nanoplexes, degradation was very slow as compared to naked siRNA indicating the inaccessibility of serum nucleases to degrade siRNA. siRNA in the form of nanoplexes was stable even after extensive incubation with serum. Both, polyplexes and lipoplexes retained more than 75% of siRNA after 24 hr. Lipoplexes, however showed more protection to siRNA as observed with gel retardation. This might be due to the incorporation of DSPE-mPEG$_{2000}$, a PEGylated lipid, which forms a shielding sheath on the lipoplexes preventing the close approach of nucleases to surface adsorbed siRNA. Protection offered by polyplexes can be attributed to the condensed structure of polyplexes that holds siRNA that is distributed inside the interior of the polyplex.

5.2.10 Salt Induced Aggregation Study

Sodium chloride was used to check the stability of nanoplexes in order to have the estimation of stability of formulations in presence of high salt concentration conditions that prevails *in vivo*.

Figure 5.34 depict changes in particle size at different concentration of sodium chloride. Increasing concentrations of sodium chloride led to increase in particle size in case of both polyplexes as well as lipoplexes. However, the size change was prominent in case of polyplexes. This might be attributed to the sterically stabilized surface of lipoplexes. Highly hydrated PEG chains around the lipoplexes might have caused low effect of electrolyte concentration on lipoplex formulation. The effect was notable up to 2% salt concentration, beyond which particle size started increasing significantly, but remained below 200 nm (**Table 5.15** and **Figure 5.34**).

In case of polyplexes, there was a linear rise in particle size after incubation with sodium chloride up to 2% concentration; however, all polyplexes maintained particle size below 200 nm. Higher concentrations led to drastic rise in particle size. Literature reports show that after a certain concentration of salt, polyplexes start to dissociate leading to

reduction in scattering intensity up to a level of sodium chloride solution (39). However, the same was not observed with any polyplex formulations. Improved stability observed with polyplexes made of Boc-alanine and Boc-leucine modified PEI can be imputed to hydrophobically modified surface of polyplexes which would have reduced the closer approach of electrolytes. However, drastic size increase occurring at higher concentration might be due to compression of the electric double layer by salt which would induce the the hydrophobic interaction between particles causing their aggregation. Both were able to maintain size below 200 nm up to concentration of 2% only.

Table 5.15 Electrolyte induced flocculation of nanoplexes

% Concentration of NaCl	Particle size (nm)			
	AAP	**AHP**	**ALP**	**DL**
0	160.00±1.56	136.25±2.33	167.85±0.49	113.30±3.25
1	179.30±3.96	151.80±4.10	187.23±4.20	120.94±3.80
2	195.75±4.45	167.35±3.61	196.95±1.91	127.76±2.04
3	216.70±3.25	188.95±3.75	218.50±4.53	137.05±2.05
4	242.65±4.45	202.15±3.61	238.60±4.67	148.80±2.97
5	257.95±4.74	214.80±4.81	259.45±2.76	159.80±3.54

*Values are represented as mean±SD, n=3.

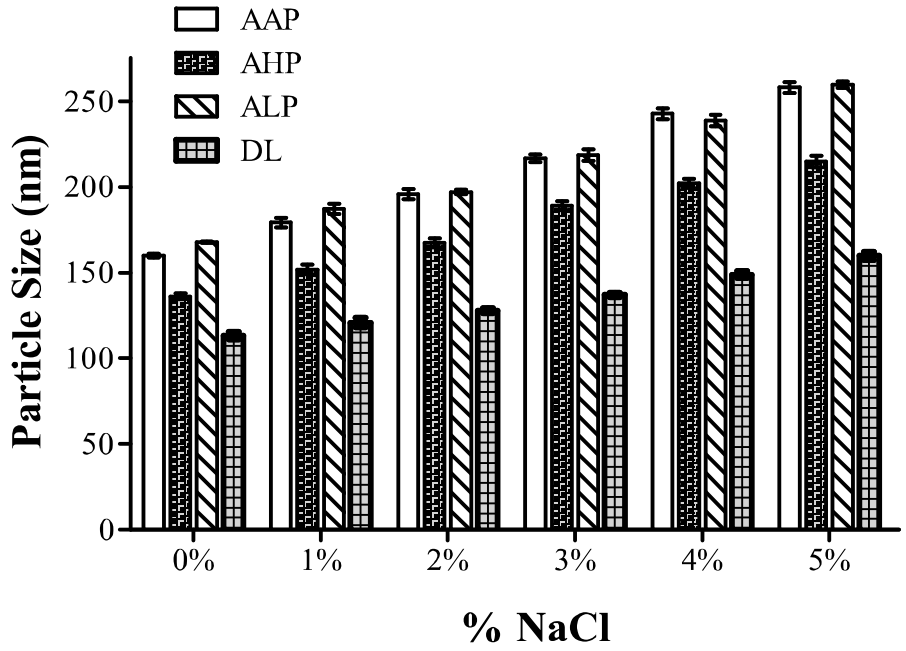

Figure 5.34 Electrolyte induced flocculation of nanoplexes.

5.2.11 Stability Study in Bronchoalveolar Lavage Fluid

Stability of nanoplexes in presence of BAL fluid was evaluated using gel electrophoresis. siRNA band density for formulations incubated for different time periods with BALF relative to that at 0 min time point was determined and % siRNA retained were calculated (**Table 5.16** and **Figure 5.35**). In presence of BAL fluid, mean siRNA retained in formulations was found to be decreasing indicating that siRNA was released in presence of BAL fluid with a loss of 4-6% after 2 hr (**Figure 5.35**). This can be attributed to the surfactants as well as negatively charged proteins present in the BAL fluid that might have affected the displacement of complexed siRNA. However, the decrease in siRNA retention at each time point was non-signficant depicting the stability of complex in presence of BAL fluid.

Table 5.16 Stability of nanoplexes in BAL fluid

Formulation	% siRNA retained							
	Time (min)							
	0	15	30	45	60	75	90	120
AAP	100	99.45± 1.52	98.85± 2.15	98.15± 1.86	96.68± 2.52	95.51± 3.45	95.49± 4.01	94.05± 1.65
AHP	100	99.76± 2.52	98.26± 1.68	97.72± 3.05	97.32± 1.96	97.21± 1.02	96.85± 0.75	96.45± 2.27
ALP	100	98.94± 2.36	98.75± 1.08	97.09± 2.00	96.84± 1.42	96.52± 0.91	96.56± 0.45	94.66± 2.01
DL	100	99.45± 1.36	99.50± 1.25	98.57± 2.06	97.96± 2.45	97.45± 1.85	96.79± 3.05	96.65± 2.36

*Values are represented as mean±SD, n=3.

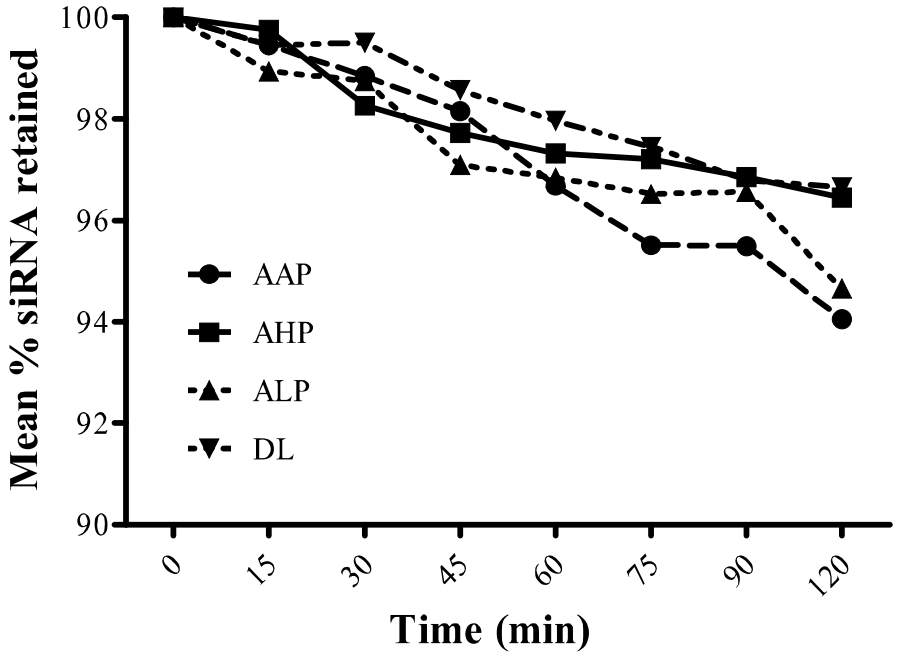

Figure 5.35 siRNA retained in nanoplexes after incubation with BALF.

However, the release was of very low amplitude for each formulation, as observed by similar siRNA band densities obtained for formulations exposed to BAL fluid. Among modified PEIs, Boc-histidine-PEI polyplexes (AHP) showed the lowest siRNA degradation. This can be attributed to partial ionization of imidazole nitrogen of Boc-histidine modified

PEI which will help condense siRNA better than Boc-leucine and Boc-alanine modified PEIs. DL showed better protection against BALF fluid, even higher than polyplexes. This might be due to better protection provided by PEGylated surface of lipoplexes against BAL fluid components by providing a steric barrier around the lipoplexes.

From the results of the BAL fluid stability study, developed nanoplexes were found to be stable in presence of pulmonary fluids.

5.2.12 Transmission Electron Microscopy

Cryo TEM of DL lipoplexes revealed that prepared lipoplexes were spherical in shape as shown in **Figure 5.36**. All vesicles were unilamellar in structure and having particle size below 200 nm. Bilayer thickness was also measured and found to be in between 5-10 nm in size. Obtained TEM images are in concordance with the data obtained from particle size analyser and it confirmed that developed polyplex particles were spherical in shape and less than 200 nm in size (**Figure 5.37**).

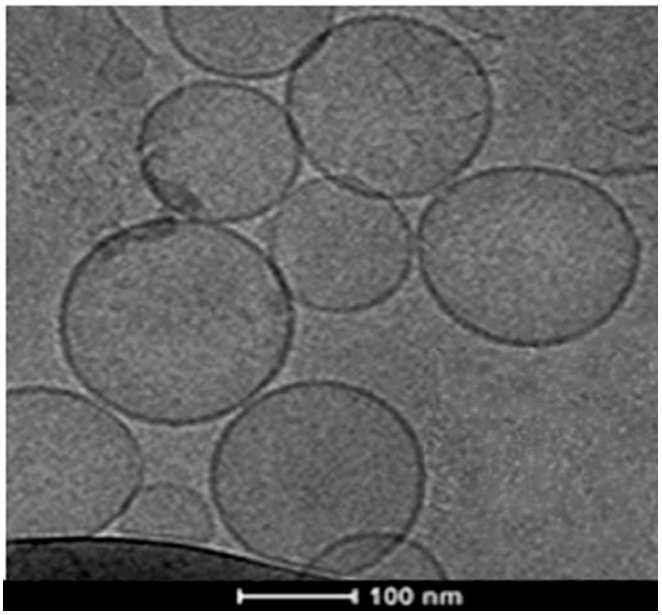

Figure 5.36 Cryo-TEM image of DL.

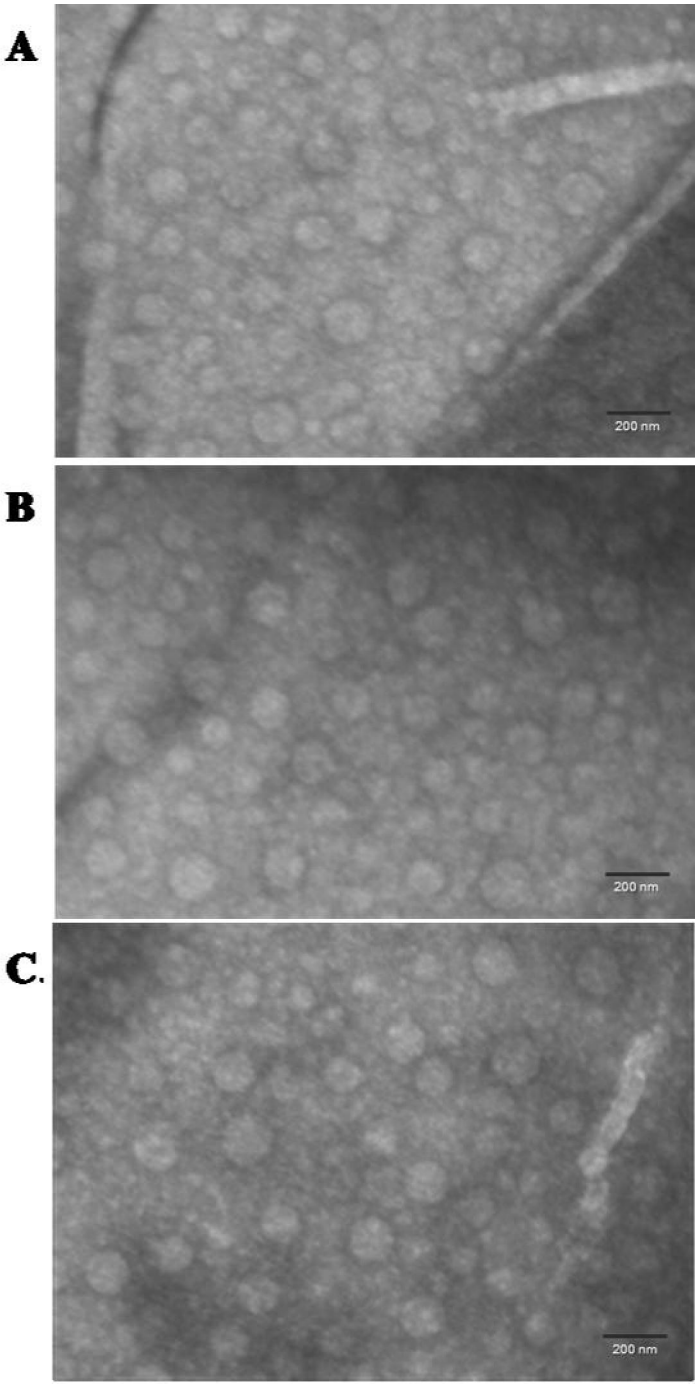

Figure 5.37 TEM images of AAP (A), AHP (B) and ALP (C).

5.3 References

1. Mintzer MA, Simanek EE. Nonviral vectors for gene delivery. Chem Rev. 2009;109(2):259-302.

2. Segura T, Shea LD. MATERIALS FOR NON-VIRAL GENE DELIVERY. Annual Review of Materials Research. 2001;31(1):25-46.

3. Lungwitz U, Breunig M, Blunk T, Gopferich A. Polyethylenimine-based non-viral gene delivery systems. European journal of pharmaceutics and biopharmaceutics : official journal of Arbeitsgemeinschaft fur Pharmazeutische Verfahrenstechnik eV. 2005;60(2):247-66.

4. Plautz SA, Boanca G, Riethoven JJ, Pannier AK. Microarray analysis of gene expression profiles in cells transfected with nonviral vectors. Molecular therapy : the journal of the American Society of Gene Therapy. 2011;19(12):2144-51.

5. Nabel GJ, Nabel EG, Yang ZY, Fox BA, Plautz GE, Gao X, et al. Direct gene transfer with DNA-liposome complexes in melanoma: expression, biologic activity, and lack of toxicity in humans. Proceedings of the National Academy of Sciences of the United States of America. 1993;90(23):11307-11.

6. Ledley FD. Nonviral gene therapy: the promise of genes as pharmaceutical products. Human gene therapy. 1995;6(9):1129-44.

7. Mok H, Lee SH, Park JW, Park TG. Multimeric small interfering ribonucleic acid for highly efficient sequence-specific gene silencing. Nat Mater. 2010;9(3):272-8.

8. Vader P, Aa L, Engbersen JJ, Storm G, Schiffelers R. Physicochemical and Biological Evaluation of siRNA Polyplexes Based on PEGylated Poly(amido amine)s. Pharmaceutical research. 2012;29(2):352-61.

9. Moret I, Esteban Peris J, Guillem VM, Benet M, Revert F, Dasi F, et al. Stability of PEI-DNA and DOTAP-DNA complexes: effect of alkaline pH, heparin and serum. Journal of controlled release : official journal of the Controlled Release Society. 2001;76(1-2):169-81.

10. Lauer SA, Nolan JP. Development and characterization of Ni-NTA-bearing microspheres. Cytometry. 2002;48(3):136-45.

11. Jauniaux E, Watson AL, Hempstock J, Bao YP, Skepper JN, Burton GJ. Onset of maternal arterial blood flow and placental oxidative stress. A possible factor in human early pregnancy failure. Am J Pathol. 2000;157(6):2111-22.

12. Phillips PG, Birnby LM, Narendran A. Hypoxia induces capillary network formation in cultured bovine pulmonary microvessel endothelial cells. Am J Physiol. 1995;268(5 Pt 1):L789-800.

13. Pugh CW, Ratcliffe PJ. Regulation of angiogenesis by hypoxia: role of the HIF system. Nat Med. 2003;9(6):677-84.

14. Hiwatashi K, Ueno S, Abeyama K, Kubo F, Sakoda M, Maruyama I, et al. A novel function of the receptor for advanced glycation end-products (RAGE) in association with tumorigenesis and tumor differentiation of HCC. Ann Surg Oncol. 2008;15(3):923-33.

15. Akakura N, Kobayashi M, Horiuchi I, Suzuki A, Wang J, Chen J, et al. Constitutive expression of hypoxia-inducible factor-1alpha renders pancreatic cancer cells resistant to apoptosis induced by hypoxia and nutrient deprivation. Cancer research. 2001;61(17):6548-54.

16. Bolcato-Bellemin AL, Bonnet ME, Creusat G, Erbacher P, Behr JP. Sticky overhangs enhance siRNA-mediated gene silencing. Proc Natl Acad Sci U S A. 2007;104(41):16050-5.

17. Mok H, Park TG. Self-crosslinked and reducible fusogenic peptides for intracellular delivery of siRNA. Biopolymers. 2008;89(10):881-8.

18. Danielsen S, Strand S, de Lange Davies C, Stokke BT. Glycosaminoglycan destabilization of DNA-chitosan polyplexes for gene delivery depends on chitosan chain length and GAG properties. Biochim Biophys Acta. 2005;1721(1-3):44-54.

19. Poole AR. Proteoglycans in health and disease: structures and functions. Biochem J. 1986;236(1):1-14.

20. Dykxhoorn DM, Palliser D, Lieberman J. The silent treatment: siRNAs as small molecule drugs. Gene therapy. 2006;13(6):541-52.

21. Layzer JM, McCaffrey AP, Tanner AK, Huang Z, Kay MA, Sullenger BA. In vivo activity of nuclease-resistant siRNAs. RNA. 2004;10(5):766-71.

22. Mahato RI, Kawabata K, Takakura Y, Hashida M. In vivo disposition characteristics of plasmid DNA complexed with cationic liposomes. Journal of drug targeting. 1995;3(2):149-57.

23. McCaffrey AP, Meuse L, Pham TT, Conklin DS, Hannon GJ, Kay MA. RNA interference in adult mice. Nature. 2002;418(6893):38-9.

24. Moret I, Esteban Peris J, Guillem VM, Benet M, Revert F, Dasi F, et al. Stability of PEI-DNA and DOTAP-DNA complexes: effect of alkaline pH, heparin and serum. J Control Release. 2001;76(1-2):169-81.

25. Minakuchi Y, Takeshita F, Kosaka N, Sasaki H, Yamamoto Y, Kouno M, et al. Atelocollagen-mediated synthetic small interfering RNA delivery for effective gene silencing in vitro and in vivo. Nucleic acids research. 2004;32(13):e109.

26. Lin W, Coombes AG, Garnett MC, Davies MC, Schacht E, Davis SS, et al. Preparation of sterically stabilized human serum albumin nanospheres using a novel Dextranox-MPEG crosslinking agent. Pharmaceutical research. 1994;11(11):1588-92.

27. Tadros ThF, Vincent B. Encyclopedia of Emulsion Technology. Becher P, editor. New York: Marcel Dekker; 1983.

28. Tadros TF. Control of the properties of suspensions. Colloids and Surfaces. 1986;18(2–4):137-73.

29. Elimelech M, Jia X, Gregory J, Williams R. Particle Deposition & Aggregation: Measurement, Modelling and Simulation. US: Elsevier Inc.; 1995.

30. Rosenecker J, Naundorf S, Gersting SW, Hauck RW, Gessner A, Nicklaus P, et al. Interaction of bronchoalveolar lavage fluid with polyplexes and lipoplexes: analysing the role of proteins and glycoproteins. J Gene Med. 2003;5(1):49-60.

31. Choosakoonkriang S, Lobo BA, Koe GS, Koe JG, Middaugh CR. Biophysical characterization of PEI/DNA complexes. J Pharm Sci. 2003;92(8):1710-22.

32. Tang MX, Szoka FC. The influence of polymer structure on the interactions of cationic polymers with DNA and morphology of the resulting complexes. Gene Ther. 1997;4(8):823-32.

33. Regelin AE, Fankhaenel S, Gürtesch L, Prinz C, von Kiedrowski G, Massing U. Biophysical and lipofection studies of DOTAP analogs. Biochimica et Biophysica Acta (BBA) - Biomembranes. 2000;1464(1):151-64.

34. Parker AL, Seymour LW. Targeting of Polyelectrolyte RNA Complexes to Cell Surface Integrins as an Efficient Cytoplasmic Transfection Mechanism. Journal of Bioactive and Compatible Polymers. 2002;17(4):229-38.

35. Gabrielson NP, Pack DW. Acetylation of polyethylenimine enhances gene delivery via weakened polymer/DNA interactions. Biomacromolecules. 2006;7(8):2427-35.

36. Kunath K, von Harpe A, Fischer D, Kissel T. Galactose-PEI-DNA complexes for targeted gene delivery: degree of substitution affects complex size and transfection efficiency. Journal of controlled release : official journal of the Controlled Release Society. 2003;88(1):159-72.

37. He W, Guo Z, Wen Y, Wang Q, Xie B, Zhu S. Alginate-graft-PEI as a gene delivery vector with high efficiency and low cytotoxicity. J Biomater Sci Polym Ed. 2012;23(1-4):315-31.

38. Moghimi SM, Symonds P, Murray JC, Hunter AC, Debska G, Szewczyk A. A two-stage poly(ethylenimine)-mediated cytotoxicity: implications for gene transfer/therapy. Molecular therapy : the journal of the American Society of Gene Therapy. 2005;11(6):990-5.

39. Zintchenko A, Philipp A, Dehshahri A, Wagner E. Simple modifications of branched PEI lead to highly efficient siRNA carriers with low toxicity. Bioconjugate chemistry. 2008;19(7):1448-55.

40. Sunshine JC, Akanda MI, Li D, Kozielski KL, Green JJ. Effects of base polymer hydrophobicity and end-group modification on polymeric gene delivery. Biomacromolecules. 2011;12(10):3592-600.

41. van der Woude I, Visser HW, ter Beest MB, Wagenaar A, Ruiters MH, Engberts JB, et al. Parameters influencing the introduction of plasmid DNA into cells by the use of synthetic amphiphiles as a carrier system. Biochimica et biophysica acta. 1995;1240(1):34-40.

42. Thomas M, Klibanov AM. Enhancing polyethylenimine's delivery of plasmid DNA into mammalian cells. Proceedings of the National Academy of Sciences. 2002;99(23):14640-5.

43. Stegmann T, Legendre J-Y. Gene transfer mediated by cationic lipids: lack of a correlation between lipid mixing and transfection. Biochimica et Biophysica Acta (BBA) - Biomembranes. 1997;1325(1):71-9.

44. Shangguan T, Pak CC, Ali S, Janoff AS, Meers P. Cation-dependent fusogenicity of an N-acyl phosphatidylethanolamine. Biochimica et Biophysica Acta (BBA) - Biomembranes. 1998;1368(2):171-83.

45. Shabani M, Hemmati S, Hadavi R, Amirghofran Z, Jeddi-Tehrani M, Rabbani H, et al. Optimization of gene transfection in murine myeloma cell lines using different transfection reagents. Avicenna Journal of Medical Biotechnology. 2010;2(3):123.

46. Rejman J, Bragonzi A, Conese M. Role of clathrin-and caveolae-mediated endocytosis in gene transfer mediated by lipo-and polyplexes. Molecular Therapy. 2005;12(3):468-74.

47. Dutta T, Agashe HB, Garg M, Balakrishnan P, Kabra M, Jain NK. Poly (propyleneimine) dendrimer based nanocontainers for targeting of efavirenz to human monocytes/macrophages in vitro. Journal of drug targeting. 2007;15(1):89-98.

48. Xu Y, Szoka FC, Jr. Mechanism of DNA release from cationic liposome/DNA complexes used in cell transfection. Biochemistry. 1996;35(18):5616-23.

49. Zelphati O, Szoka FC. Mechanism of oligonucleotide release from cationic liposomes. Proceedings of the National Academy of Sciences. 1996;93(21):11493-8.

50. Zhou X, Huang L. DNA transfection mediated by cationic liposomes containing lipopolylysine: characterization and mechanism of action. Biochimica et Biophysica Acta (BBA) - Biomembranes. 1994;1189(2):195-203.

51. Zuhorn IS, Bakowsky U, Polushkin E, Visser WH, Stuart MC, Engberts JB, et al. Nonbilayer phase of lipoplex-membrane mixture determines endosomal escape of genetic cargo and transfection efficiency. Molecular therapy : the journal of the American Society of Gene Therapy. 2005;11(5):801-10.

52. Švastová E, Hulíková A, Rafajová M, Zat'ovičová M, Gibadulinová A, Casini A, et al. Hypoxia activates the capacity of tumor-associated carbonic anhydrase IX to acidify extracellular pH. FEBS letters. 2004;577(3):439-45.

53. Kang HC, Samsonova O, Kang SW, Bae YH. The effect of environmental pH on polymeric transfection efficiency. Biomaterials. 2012;33(5):1651-62.

54. Kuwabara K, Ogawa S, Matsumoto M, Koga S, Clauss M, Pinsky DJ, et al. Hypoxia-mediated induction of acidic/basic fibroblast growth factor and platelet-derived growth factor in mononuclear phagocytes stimulates growth of hypoxic endothelial cells. Proceedings of the National Academy of Sciences. 1995;92(10):4606-10.

55. Lee SY, Huh MS, Lee S, Lee SJ, Chung H, Park JH, et al. Stability and cellular uptake of polymerized siRNA (poly-siRNA)/polyethylenimine (PEI) complexes for efficient gene silencing. J Control Release. 2010;141(3):339-46.

56. Van Rompaey E, Engelborghs Y, Sanders N, De Smedt SC, Demeester J. Interactions between oligonucleotides and cationic polymers investigated by fluorescence correlation spectroscopy. Pharm Res. 2001;18(7):928-36.

57. Jones NA, Hill IR, Stolnik S, Bignotti F, Davis SS, Garnett MC. Polymer chemical structure is a key determinant of physicochemical and colloidal properties of polymer-DNA complexes for gene delivery. Biochim Biophys Acta. 2000;1517(1):1-18.

58. Quinn DA GH. Hyaluronan in acute lung injury. In: Vincent J-L, editor. Yearbook of Intensive Care and Emergency Medicine: Berlin: Springer Berlin/Heidelberg; 2006.

59. Judge AD, Bola G, Lee AC, MacLachlan I. Design of noninflammatory synthetic siRNA mediating potent gene silencing in vivo. Mol Ther. 2006;13(3):494-505.